

Structure-based Discovery of a Series of NSD2-PWWP1

Inhibitors

Na Li,^{1,5,#} Hong Yang,^{2,#} Ke Liu,^{3,#} Liwei Zhou,^{1,#} Yuting Huang,² Danyan Cao,¹
Yanlian Li,¹ Yaoliang Sun,⁴ Aisong Yu,² Zhiyan Du,¹ Feng Yu,³ Ying Zhang,²
Bingyang Wang,⁴ Meiyu Geng,^{2,6} Jian Li,⁷ Bing Xiong,^{1,5,*} Shilin Xu,^{4,*} Xun
Huang,^{2,6,*} Tongchao Liu^{1,*}

¹*Department of Medicinal Chemistry, Shanghai Institute of Materia Medica, Chinese Academy of Sciences, 555 Zuchongzhi Road, Shanghai 201203, P. R. China*

²*Division of Antitumor Pharmacology, State Key Laboratory of Drug Research, Shanghai Institute of Materia Medica, Chinese Academy of Sciences, 555 Zuchongzhi Road, Shanghai 201203, P. R. China*

³*Shanghai Synchrotron Radiation Facility, Shanghai Advanced Research Institute, Chinese Academy of Sciences, 239 Zhangheng Road, Shanghai 201210, China*

⁴*Department of Medicinal Chemistry, State Key Laboratory of Drug Research, Shanghai Institute of Materia Medica, Chinese Academy of Sciences, #555 ZuChong Zhi Road, Shanghai, 201203, China*

⁵*University of Chinese Academy of Sciences, NO.19A Yuquan Road, Beijing 100049, P. R. China*

⁶*Hangzhou Institute for Advanced Study, UCAS, Hangzhou 310024, P. R. China;*

⁷*College of Pharmaceutical Sciences, Gannan Medical University, Ganzhou 341000, China*

[#]These authors contributed equally

*Corresponding authors. Tel: +86 21 50806600 ext. 5412 fax: +86 21 50807088.

Email: (T. L.) tongchao_liu@simm.ac.cn; (X.H.) xhuang@simm.ac.cn; (S.X.)

slxu@simm.ac.cn; (B. X.) bxiong@simm.ac.cn

ABSTRACT

Overexpression, point mutations or translocations of protein lysine methyltransferase NSD2 was occurred in many types of cancer cells. Therefore, it was recognized as onco-protein and considered as a promising anticancer drug target. NSD2 consists of a SET catalytic domain and two PWWP domains binding to methylated histone proteins. Here, we reported our efforts to develop a series of NSD2-PWWP1 inhibitors, and further structure-based optimization resulted a potent inhibitor **38**, which has the high selectivity towards NSD2-PWWP1 domain. The detailed biological evaluation revealed that compound **38** can bind to NSD2-PWWP1 and then affect the expression of genes regulated by NSD2. The current discovery will provide a useful chemical probe to the future research in understanding the specific regulation mode of NSD2 by PWWP1 recognition, and pave the way to develop potential drugs targeting NSD2 protein.

Keywords: Epigenetics; NSD2; PWWP domain; Inhibitor; Structure-based drug discovery

INTRODUCTION

The nuclear receptor-binding SET domain (NSD) family of protein lysine methyltransferases consists of three members: NSD1, NSD2 and NSD3, and which

predominantly catalyzes the mono- and di-methylation of histone 3 lysine 36 (H3K36).¹ High expression, point mutations or translocations of NSD family frequently occurred in multiple types of human cancers. NSD2, also known as MMSET (multiple myeloma SET domain) or WHSC1 (Wolf-Hirschhorn syndrome candidate 1) is involved in several cellular processes, including DNA damage repair, epithelial–mesenchymal transformation (EMT) and cell cycle regulation, and was identified as an important driver in oncogenesis.² Notably, NSD2 is closely related to accelerated disease progression and rapid relapse in 15–20% of multiple myeloma (MM) harboring the t(4;14) chromosomal translocation with increased levels of H3K36me₂,³ and among the most frequently mutated genes in pediatric cancer genomes, E1099K mutant of NSD2 is hyperactivated in acute lymphoblastic leukemia.⁴ Recent studies have revealed that overexpression of NSD2 occurred in several solid tumors including bladder, prostate, glioblastoma and gastrointestinal.^{5,6}

NSD2 is a multi-domain protein, consists of the SET domain performing the catalytic methylation function and two PWWP (proline-tryptophan-tryptophan-proline) domains. The N-terminal PWWP domain (PWWP1) acts as the reader domain that preferentially binds to the nucleosomes containing H3K36me₂ while PWWP2 domain can bind to histone H3K36/79me₃ and dsDNA. Though PWWP1 and PWWP2 are different in affinity to histone substrates, they have been reported to cooperate in maintaining appropriate nuclear localization. This process relies on the conserved aromatic cage consists of PWWP1 Y233, W236 and F266, which are orthogonally positioned and interact with the methylated side chain of H3K36 residue. The

NSD2-PWWP1:H3K36me2 interaction plays a critical role in stabilizing NSD2 at chromatin, and then facilitates epigenetic spreading and propagation of H3K36me2 which is required for the recruitment of DNMT3A and maintenance of DNA methylation at intergenic regions for gene transcription.⁷ In carcinoma cells, H3K36me2 signal alteration underlies epithelial-to-mesenchymal transition and mesenchymal-to-epithelial transition that is critical for metastatic.⁸

Since NSD2 is a promising target for targeted cancer therapy, several groups have reported their efforts in developing selective small-molecule inhibitors targeting the catalytic domain or the PWWP domains of NSD proteins (Figure 1). Huang et al. screened a fragment library of approximately 1600 fragment-like compounds against SET domain of NSD1 with 2D-NMR experiments and found 6-chloro-1,3-benzothiazol-2-amine that binds to the SET domain.⁹ Further structure-based optimization was conducted and resulted to a covalent inhibitor BT5 (**1**) with moderate selectivity over NSD2 and NSD3. Bottcher et al. from Boehringer Ingelheim company adopted the fragment-based strategy to identify hits to the PWWP1 domain of NSD3.¹⁰ BI-9321(**2**) was discovered as a potent and selective inhibitor of NSD3-PWWP1 domain, with IC₅₀ value of 0.2 μM in the TR-FRET assay. Coussens et al. utilized the high-throughput screening to identify five small-molecules as inhibitors of the catalytic SET domain and compound **3** exhibited apparent activity in cells.¹¹ Freitas et al. reported the first inhibitor (**4**) of NSD2-PWWP1 domain with K_d value about 3.4 μM in an SPR assay, which could abrogate histone H3K36me2 binding to the PWWP1 domain in cells with an IC₅₀ of 17.3 μM.¹² Lately, Dilworth et

al. continued their previous work and discovered a more potent inhibitor UNC6934 ($K_d=91$ nM), which harbors same chemical scaffold as compound **4**.¹³

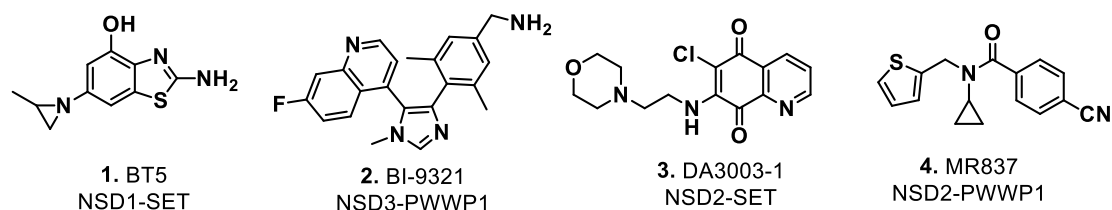


Figure 1. Representative small-molecule inhibitors of NSD1-3 proteins.

Since there is only one chemotype of NSD2-PWWP1 inhibitors that showed biological activity, therefore, more diverse chemical scaffolds and potent NSD2-PWWP1 inhibitors are needed to further assess the pharmacological potential of NSD2. Herein, we reported our effort to conduct a structure-based optimization of NSD2-PWWP1 ligands, leading to a selective NSD2-PWWP1 inhibitor **38** with significantly improved potency. Compound **38** can clearly bind to NSD2-PWWP1 and further affect the expression of genes regulated by NSD2. We believe that the discovery and related biological evaluation will contribute to the further research of the specific regulation mode of NSD2 by PWWP1 recognition, and furthermore, our discovery also provided a certain material basis for the functional study of NSD2.

RESULTS AND DISCUSSION

Rational Design of Selective NSD2-PWWP1 Inhibitors.

At the initial stage of this project, we analyzed the binding model of reported small-molecule compounds to understand the binding basis between inhibitors and proteins, which enabled us to rationally design a new class of NSD2 inhibitors.

Currently, the crystal structure of NSD2-PWWP1 domain bound with MR837 was reported (PDB ID: 6UE6)¹², which revealed two important binding features: 1) N-cyclopropyl amide of MR837 occupied the aromatic cage sub-pocket forming by three conservative aromatic residues, Tyr233, Trp236 and Phe266; 2) an essential hydrogen bonding interaction between Ala270 residue and the N atom of benzonitrile. As mentioned above, BI-9321, the first selective and potent PWWP inhibitor in NSD family was reported by Bottcher et al. and demonstrated in the cocrystal structure (PDB code: 6G2O)¹⁰, binds to NSD3-PWWP1 domain by the following patterns: the aromatic cage was occupied by N-methylimidazole ring; the N atom in the quinoline ring interacted with Ser314 through hydrogen bonding; and the NH₂ of benzylamine extending out the binding pocket and forming a strong electrostatic interaction with nearby negative charged residue Glu318.

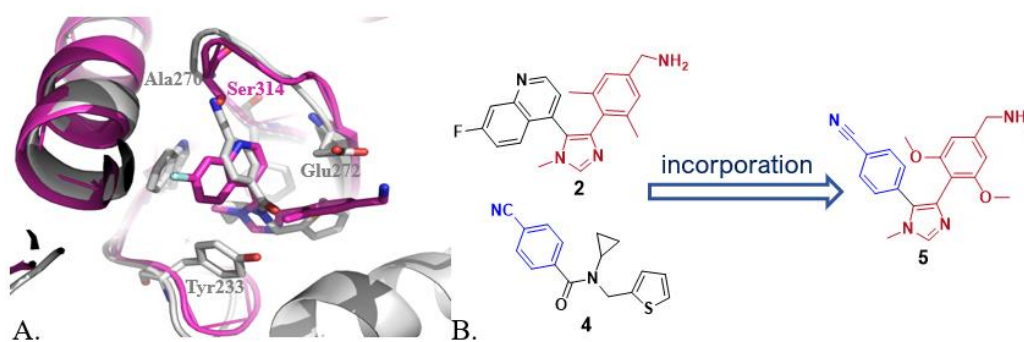


Figure 2. Design of NSD2-PWWP1 inhibitor. (A) The superimposition of crystal structures of PWWP inhibitors of NSD2-PWWP1 (MR837, PDB code 6UE6, colored gray) and NSD3-PWWP1 (BI-9321, PDB code 6G2O, colored purple). (B) Design of new chemotype of NSD2-PWWP1 inhibitor **5**.

By superposition of these two cocrystal structures (Figure 2A), it could be seen that, comparing the binding site of NSD3-PWWP1 domain with the NSD2-PWWP1

domain, the most striking difference is at the vicinity of benzonitrile group of MR837. In the NSD2-PWWP1 domain, there are Gly268, Asp269 and Ala270 residues forming hydrogen bonds with benzonitrile structure, while in NSD3-PWWP1 domain, at the same position, there are Ser314, Asn315 and Gln316 surrounding the quinolone ring of BI-9321. It should be noted that the side chain of Ser314 forming a hydrogen bond with the nitrogen atom of quinoline, which would impede the benzonitrile group binding. Therefore, we rationally designed the new chemotype of NSD2-PWWP1 inhibitors by incorporating the benzonitrile into the BI-9321 to replace the quinoline ring, which was thought that could achieve the binding selectivity of NSD2 over the NSD3 protein. Besides, we also noticed that the methyl group on the benzene ring of BI-9321 was at the similar position of the O atom of the amide group of MR837, and the distance between the methyl C atom on the benzene ring of BI-9321 and Tyr233 was 3.6 Å. We hypothesized that if the methyl on the benzene ring was replaced with methoxy group, the O atom of methoxyl group may be able to form a hydrogen bond with Tyr233. Taking together, we designed and synthesized compound **5** in Figure 2B for the biological test to verify the design strategy.

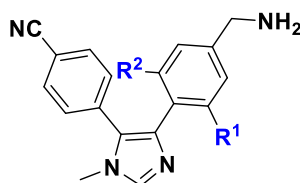
Structure-Activity Relationship (SAR) Exploration and Optimization of Ligands.

As shown in Table 1, compound **5** with two methoxy groups displayed a good binding affinity to NSD2 PWWP1 domain, with an IC₅₀ value of 4.44 μM, which is much better than MR837 (**4**). This encouraged us to synthesize analogs **6 - 12**. According to the binding assay, removal of one or two methoxy groups led to compounds **6** and **7**

showing slightly reduced potency with IC₅₀ values of 11.97 μM and 13.95 μM, respectively. When mono-halogen groups such as chlorine and fluorine were introduced (compound **8** and **9**), they also slightly reduced potency if comparison with compound **5**. However, single trifluoromethyl-substituent and methyl-substituent compounds (**10** and **11**) showed equal potency to compound **5**. When another methyl group was introduced to yield compound **12**, the potency was significantly improved to an IC₅₀ value of 0.57 μM, about 8-fold more potent than of compound **5**. This encouraged us to further explore the effect of other parts of this chemotype inhibitors on NSD2-PWWP1 binding.

Table 1. NSD2 Inhibition of Compounds 5 - 12 Combining R¹- and R²-

Substituents^a



compound	R ¹ =	R ² =	NSD2 (IC ₅₀ , μM)
5	OCH ₃	OCH ₃	4.44 ± 3.30
6	OCH ₃	H	11.97 ± 3.64
7	H	H	13.95 ± 6.73
8	Cl	H	6.11 ± 3.38
9	F	H	11.19 ± 2.80
10	CF ₃	H	6.01 ± 2.02
11	CH ₃	H	4.68 ± 2.12

12	CH ₃	CH ₃	0.57 ± 0.12
MR837	-	-	24.67 ± 1.86

^aIC₅₀ values are shown as the mean ± SD from at least two separate determinations.

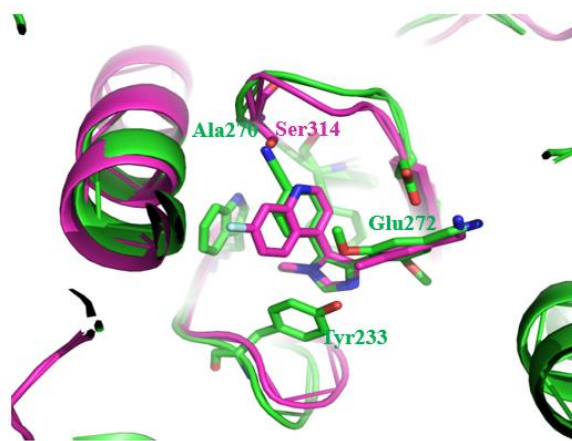


Figure 3. Superimposition of the crystal structure of NSD2-PWWP1 domain with compound **5** (colored green, PDB ID: 7VLN) and the crystal structure of NSD3-PWWP1 bound with BI-9321 (colored purple, PDB ID: 6G2O).

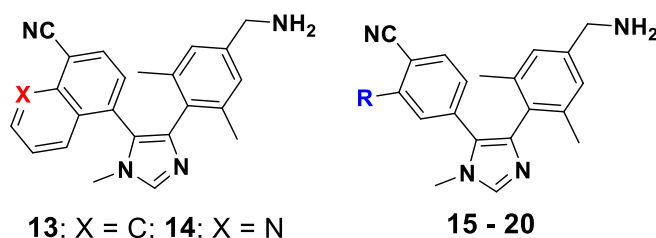
To verify the design, we performed the crystallization experiment and solved the cocrystal structure of NSD2-PWWP1 domain with compound **5**. As illustrated in Figure 3, compound **5** bound to the NSD2 in a mode very similar to BI-9321 bound to the NSD3: the N-methylimidazole situated into the aromatic cage and the benzylamine group interacted with the nearby Glu272; while the benzonitrile motif represents as an essential pharmacophore for PWWP1 of NSD2, which, as predicted, interacts with residues Asp269 and Ala270. Clearly, the nitrile group would be collided with the serine residue in NSD3.

Based on this solved structure, we next conducted a series of structural modifications to get compounds **13** – **20** to further explore the interactions with this

benzonitrile binding subpocket. As shown in Table 2, replacement of the benzonitrile core of compound **12** with a naphthonitrile moiety led to compound **13** showing analogous potency with an IC₅₀ value of 0.52 μM. Further replacement of the naphthalene moiety with a quinoline moiety generated compound **14** showing an IC₅₀ value of 1.58 μM, 3-fold less potent than compound **13**. Introducing an amino- or methylamino-substituent in the ortho-position of cyano group of compound **12** reduced the potency (compound **15** and **16**). Introduction of other small substituents afforded compounds **17** – **20**. Unfortunately, all these compounds exhibited less activity against NSD2. These results indicate that limited structural variations are tolerated in this region and the naphthonitrile framework remains to be advantageous to interact with NSD2. Because compound **13** is slightly more potent, and protein thermal shift assay (TSA) experiment further confirmed that compound **13** can selectively bind to NSD2-PWWP1 protein more tightly than compound **12** (Figure S1), we selected compound **13** for further structural optimization with the central naphthonitrile core intact.

Table 2. NSD2 Inhibition of Compounds Bearing Different Aromatic

Cyano-Fragments^a



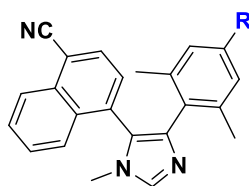
compound	R =	NSD2 (IC ₅₀ , μM)
13	-	0.52 ± 0.20

14	-	1.58 ± 0.85
15	NH ₂	8.78 ± 2.18
16	NHCH ₃	> 20
17	F	2.91 ± 0.13
18	Cl	5.03 ± 2.60
19	OCH ₃	10.93 ± 7.33
20	CF ₃	15.41 ± 1.82

^aIC₅₀ values are shown as the mean ± SD from at least two separate determinations.

From the cocrystal structure of NSD3-PWWP1 in complex with BI-9321, we can learn that the benzylamine group interacts with Glu318 residue by a hydrogen bond and this residue is conserved in the PWWP1 domain of NSD2. We synthesized and tested compounds bearing different hydrogen bond groups as the replacement of the benzylamine group. As shown in Table 3, almost all these compounds lost activity against NSD2 by showing IC₅₀ values greater than 20 μM. Notably, compounds **24** and **27** showed much reduced potency with IC₅₀ values of 13.81 μM and 10.56 μM, respectively. These results indicated that benzylamine group was necessary for activity against NSD2 and minor modifications led to much reduced potency.

Table 3. NSD2 Inhibition of Compounds Bearing Different H-bond Donor Groups^a



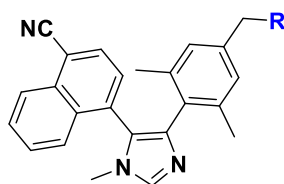
compound	R =	NSD2 (IC ₅₀ , μM)
21	CN	>20
22	CHO	>20
23	COCH ₂ CH ₃	>20
24	CH ₂ OH	13.81 ± 0.47
25	CHOHCH ₂ CH ₃	>20
26	NHBoc	>20
27	NH ₂	10.56 ± 3.31

^aIC₅₀ values are shown as the mean ± SD from at least two separate determinations.

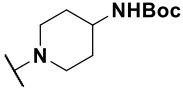
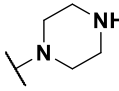
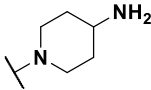
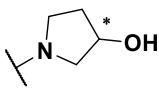
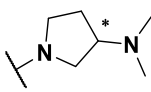
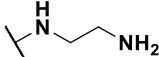
During the exploration of SARs, we found that *tert*-butoxycarbonyl-protected compound **13**, compound **28** still showed moderate potency with an IC₅₀ value of 1.67 μM. This indicated that there is certain space around this binding subsite to conduct structural modifications. Therefore, we further explored steric and hydrophilic tolerance by introducing bulky alkyl- or water-soluble substituents. As shown in Table 4, The *N*-ethyl substituted compound **29**, *N*-cyclopropyl substituted compound **30** and *N*-*tert*-butyl substituted compound **31** displayed increased potency with IC₅₀ values of 0.70 μM, 0.43 μM and 0.64 μM, respectively, which were equivalent to compound **13**. When the nitrogen was double substituted to afford compounds **32** - **36**, they showed decreased potency with IC₅₀ values ranging from 1.49 μM to 8.07 μM. However, removal of Boc protection led to significantly increased potency (compound **37** and **38**), with an IC₅₀ value of 1.89 μM and 0.11 μM, respectively. Introduction of a hydroxyl group at the C3-position of compound **32** led to 4-fold

increased potency (compound **39**), while the dimethylamino group led to retained potency (compound **40**) compared to corresponding compound **32**. Replacement of the amino piperidine of compound **38** with an ethylenediamine yielded compound **41** showing 6-fold reduced potency. Notably, among these compounds, compound **38** showed the best potency against NSD2, 5-fold more potent than compound **13**.

Table 4. NSD2 Inhibition of Compounds Bearing Variable Amino Substituents^a



compound	R =	NSD2 (IC ₅₀ , μM)
13		0.52 ± 0.20
28		1.67 ± 0.41
29		0.70 ± 0.12
30		0.43 ± 0.01
31		0.64 ± 0.10
32		2.07 ± 0.43
33		1.49 ± 0.16
34		3.84 ± 1.60
35		8.07 ± 2.37

36		8.05 ± 3.64
37		1.89 ± 1.59
38		0.11 ± 0.01
39		0.52 ± 0.10
40		2.00 ± 0.86
41		0.62 ± 0.42

^aIC₅₀ values are shown as the mean ± SD from at least two separate determinations.

Biological Evaluation

Selectivity profile with Protein Thermal shift

We carried out protein thermal shift assay to directly confirm the binding between NSD2-PWWP protein and compound **38**. As shown in Figure 4, compared to DMSO control, the melting temperature (T_m values) of NSD2-PWWP1 protein was evidently increased due to the addition of compound **38** and the change of melting temperature (T_m) in a dose-dependent manner at concentrations from 0.781 μ M to 200 mM. The results indicated that the ligands directly bind to NSD2-PWWP protein and could strengthen its stability *in vitro*. We further evaluated the target binding specificity of compound **38** using the thermal shift assay. Our results show that compound **38** exhibited remarkable selectivity against NSD2-PWWP1 protein over other PWWP domains protein (NSD3-PWWP1, DNMT3A-PWWP, ZCWPW1-PWWP).

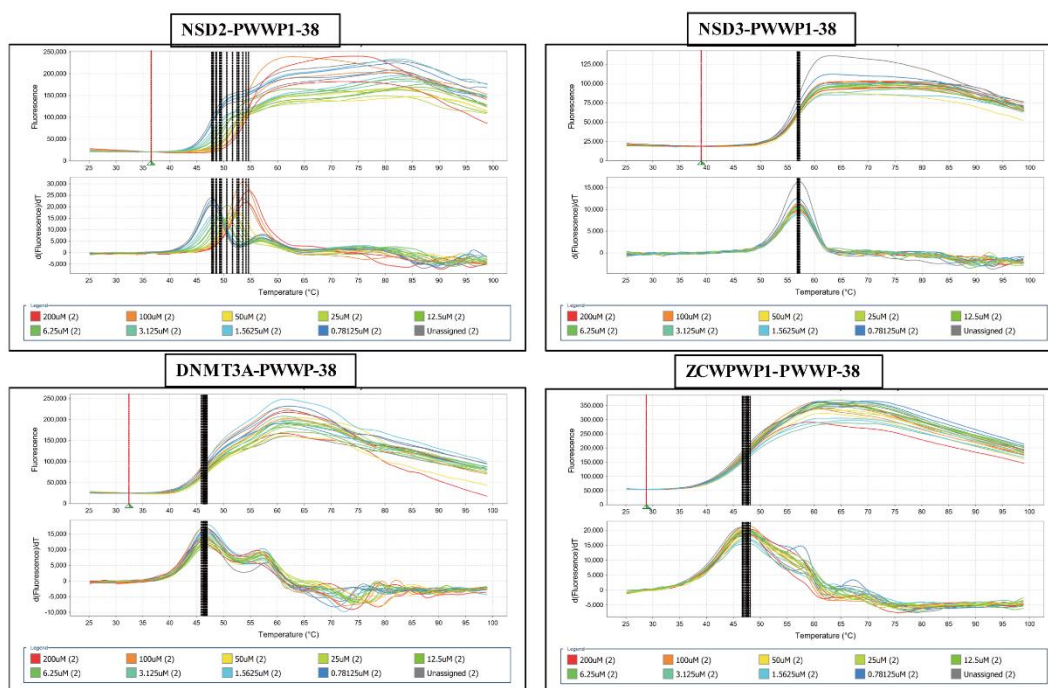


Figure 4. The melting curves of PWWP domains protein protein with compound **38**. The thermal shift assay displayed that treatment with compound **38** increases the melting temperature. Compound **38** exhibited remarkable selectivity against NSD2-PWWP1 protein over other PWWP domains protein (NSD3-PWWP1, DNMT3A-PWWP, ZCWPW1-PWWP).

Target validation at the molecular and cellular level

We proved in the previous section that compound **38** could bind to NSD2-PWWP1 domain. To further detect whether compound **38** can affect HK36me2, we adopted AlphaLisa which was designed for screening NSD2 enzymatic inhibitors. It was shown that compound **38** did not display inhibition effect on H3K36me2 *in vitro* (Figure 5A). Consistent with AlphaLisa results, compound **38** caused little effect on general H3K36me2 in cellular level (Figure 5B). These results are consistent with the findings from the study of Dilworth et al., as they pointed out that PWWP1 antagonism by UNC6934 did not have a significant effect on ribosome transcription

or global levels of H3K36me2.¹³ In conclusion, compound **38** had no impact on SET domain or enzyme activity catalytic function, which further validated that compound **38** could specifically binds to PWWP domain.

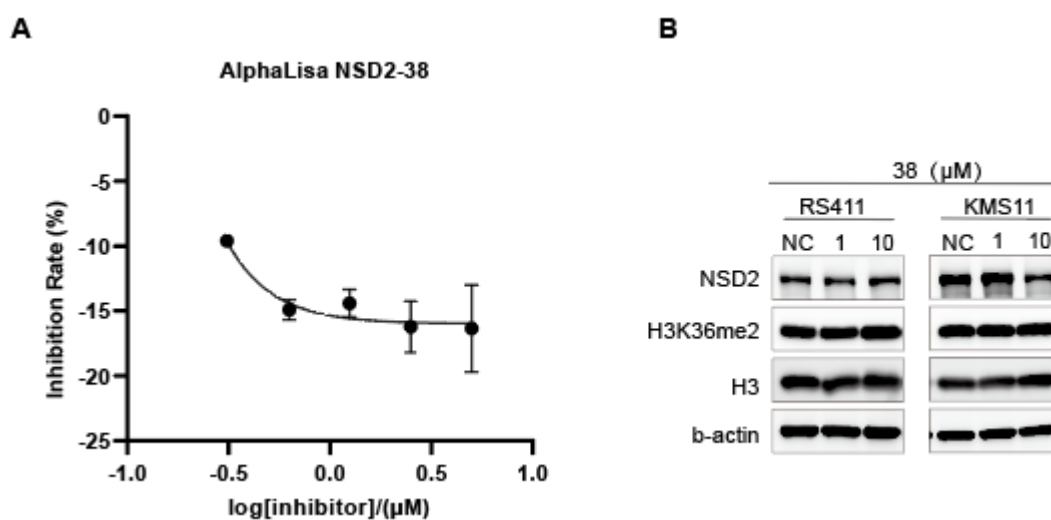
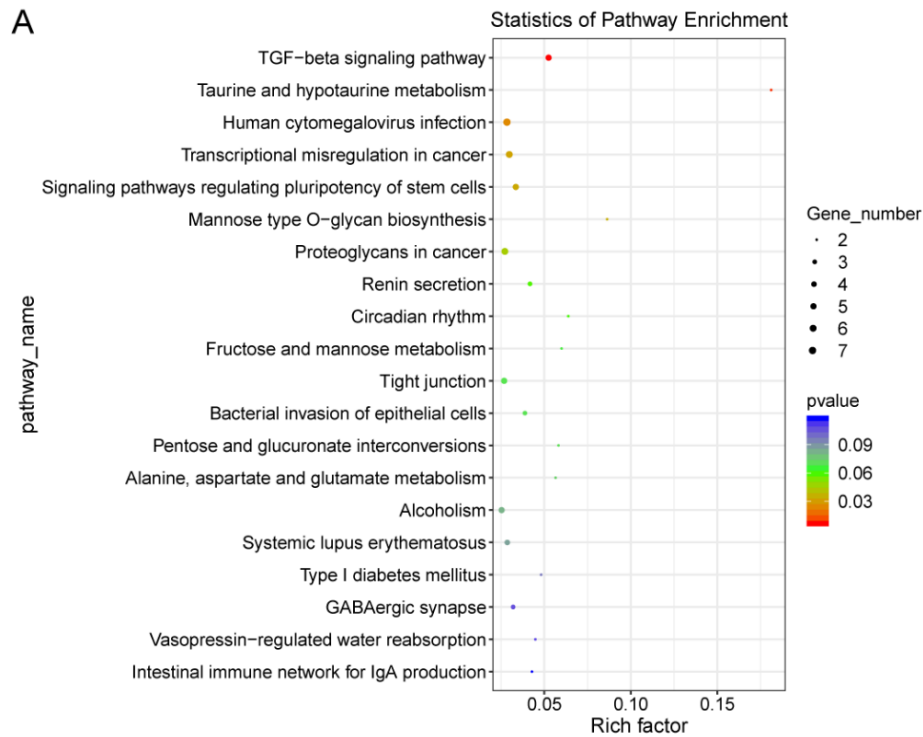


Figure 5. Target validation of compound **38** in molecular and cellular level. (A) The inhibition of compound **38** on the H3K36me2 level via AlphaLisa screening. (B) RS4:11and KMS11 cells were treated with compound **38** at gradient concentrations for 3 days, and the protein level of H3K36me2 was detected by western blot. β -actin was used as a loading control. Data are reported as the mean \pm SD.

NSD2-positive correlated downstream genes validation

To examine the cellular pathways affected by compound **38**, we performed RNA sequencing (RNA-seq) on the sensitive cell line KMS-11 by treating the cells with compound **38** or DMSO as a control for 72 h. By the KEGG analysis of the RNA-Seq, multiple cellular pathways are changed upon compound **38**. Numerous genes were adjusted up or down (Figure 6A and Figure 6B).



B

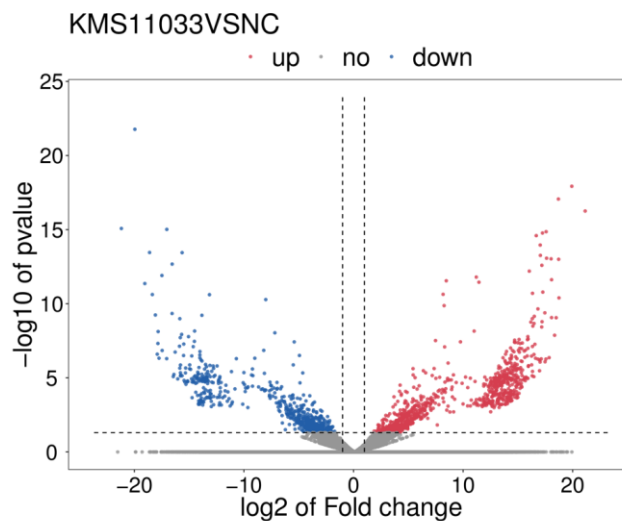


Figure 6. (A) KEGG analysis of the differential genes upon compound **38** treatment identified by RNA-seq in KMS-11 cells. (B) Volcano plot showing the differentially expressed genes in KMS-11 cells treated with compound **38** (8 μ M) for 72 h. We next determined whether compound **38** could affect NSD2 correlated downstream genes. The expression of several published representative genes (PAK1, RRAS2, TCFA, TEMEL2, HSPG2, NCAM1) were validated in two cancer cell lines by

qRT-PCR analysis. Six pairs of qPCR primers were designed. RT-PCR results showed that NSD2 target genes PAK1, RRAS2, TGFA, TEMEL2, NCAM1 remarkably decreased in compound **38** treatment group compared with control in MV4;11 and KMS11 cell lines, except for HSPG2. These results confirmed compound **38** could affect NSD2 correlated downstream genes changes (Figure 7). A previous study indicate that NSD2-PWWP1 mutation can slightly reduce H3K36me2 level.¹⁴ However, we found that interruption of NSD2 and H3K36me2 can downregulate gene transcription without influence of H3K36me2 level. These results confirm a multiple function protein of NSD2 according to its structure.

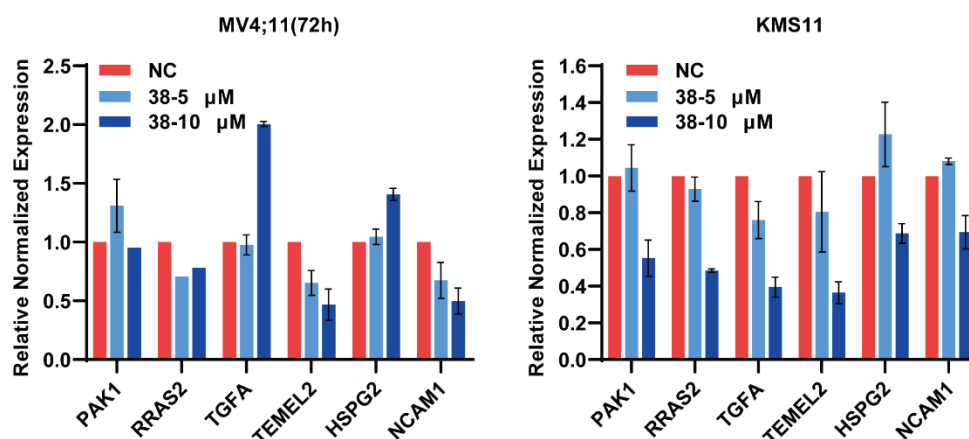


Figure 7. Downstream oncogenic transcriptional programs of compound **38**. The effects of compound **38** on gene expressions in 2 cell lines. The cell lines were treated with vary concentrations of compound **38** for 3 days. Data are reported as the mean \pm SD.

Cell-based activity

We then assessed the potential antitumor activity of compound **38** *in vitro*, we evaluated its effects on cell proliferation in a panel of human cell lines. The results demonstrated that compound **38** inhibited cell proliferation in these cell lines, including the cell line RS4:11 ($IC_{50} = 6.30 \mu M$), MV4;11 ($IC_{50} = 2.23 \mu M$), KMS11

($IC_{50} = 8.43 \mu\text{M}$), and MM1S ($IC_{50} = 10.95 \mu\text{M}$). (Figure 8). Our previous study reported a NSD2-SET domain inhibitor 9c which showed great inhibitory effect in NSD2 mutant cells KMS11 and RS4:11 (IC_{50} were $0.52 \mu\text{M}$ and $1.88 \mu\text{M}$, respectively). However, NSD2 WT cell MV4;11 showed little response to 9c.¹⁵ In this study, NSD2-PWWP1 inhibitor **38** showed inhibitory effect in both NSD2 mutant and wild type cells. Therefore, we speculated that NSD2-PWWP1 inhibitor inhibited cell proliferation independent of NSD2 genotype, which was different from NSD2-SET inhibitor.

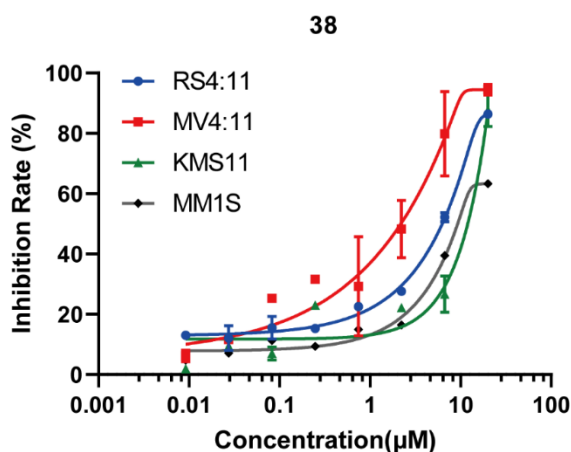


Figure 8. Cellular activity of compound **38**. The inhibitory effects on the growth of 4 cell lines treated with compound **38** at gradient concentrations for 6 days, and the inhibitory rate was measured using the CCK8 Kit. Data are reported as the mean \pm SD.

compound 38 induces apoptosis and cell cycle arrest

Next, we further investigated the effects of compound **38** on cell cycle progression and apoptosis. The effects of compound **38** on cell cycle progression and apoptosis were evaluated in KMS11 and MV4;11 cells. We treated the KMS11 and MV4;11 cells with vehicle alone or compound **38** at 5 and 10 μM for 72 h and

evaluated by flow cytometry. A higher proportion of apoptotic cells was observed after compound **38** treatment among the KMS11 and MV4:11 cells and the apoptotic effect is dose-dependent (Figure 9A). Moreover, cell cycle analysis showed that treatment of compound **38** in the KMS11, and MV4:11 cells increased the proportions of cells in G0/G1 phase whereas decreased the proportions of cells in S and G2/M phase (Figure 9B).

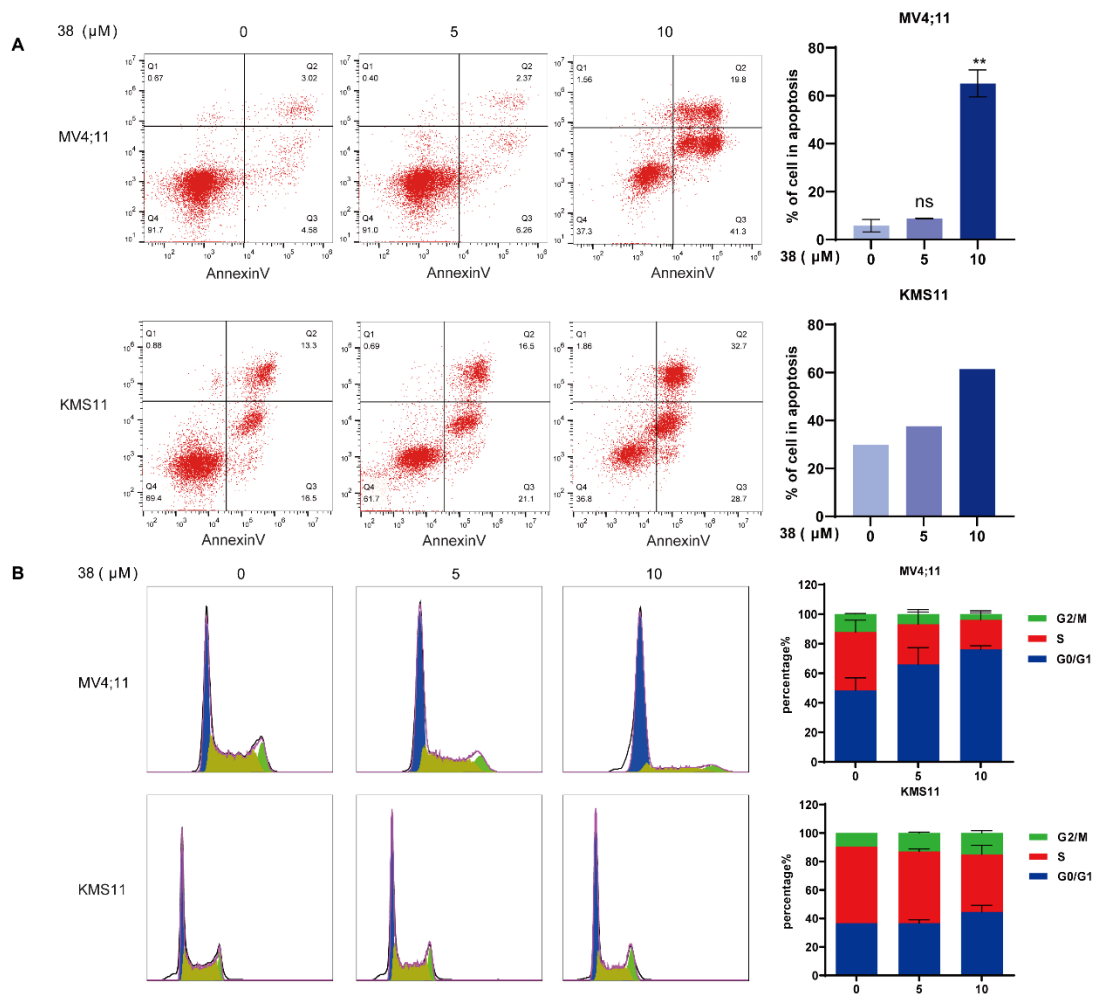


Figure 9. compound **38** induces cell apoptosis and arrests the cell cycle at the G0/G1 phase in MV4:11 and KMS11 cells. (A) KMS11 and MV4:11 cells were treated with various concentrations **38** (at 5 and 10 μM) for 72 h, and the effects on apoptosis were examined by flow cytometry. (B) KMS11 and MV4:11 cells were incubated with **38** (at 5 and 10 μM) for 24 h, and the the percentage of each cell cycle

phase were determined by flow cytometry.

CHEMISTRY

The synthesis of compounds **5** – **12** is depicted in Scheme 1. The starting materials 1-methyl-1*H*-imidazole (**42**) and 4-bromobenzonitrile (**43**) were coupled to afford intermediate **44** via palladium acetate-catalyzed reaction. The intermediate **44** was reacted with NBS to provide the key intermediate **45**, which was then subjected to Suzuki coupling with corresponding boronic acid or boronic acid pinacol ester to provide intermediates **46** – **48** and **49** – **53**. Finally, the intermediates **46** – **48** underwent reductive amination reaction to obtain the target compounds **5** - **6** and **12**, and the target compounds **7** - **11** were achieved from **49** – **53** by Boc-deprotection.

The synthesis of compounds **13** – **14** and **28** were similar to those described for **5** and **7**, as illustrated in Scheme 2. The reaction of 1-methyl-1*H*-imidazole (**42**) and **59a-b** produced intermediates **60a-b**, which was further treated with NBS to afford intermediates **61a-b**. The target compound **28** was obtained by Suzuki coupling of **61a** and **58e**, and the target compound **13** was achieved by Boc-deprotection of compound **28**. Coupling of **61a** with **55c**, followed by reductive amination produced the target compound **14**.

The synthesis of compounds **15** and **16** is shown in Scheme 3. The commercially available 2-amino-4-bromobenzonitrile (**64a**) was converted to intermediate **64b** by treatment with iodomethane. The starting materials 4-bromo-1-methyl-1*H*-imidazole (**63**) was coupled with 4-bromobenzonitrile derivatives (**64a-b**) to afford intermediates **65a-b** via palladium acetate-catalyzed reaction. The intermediates **65a-b** were

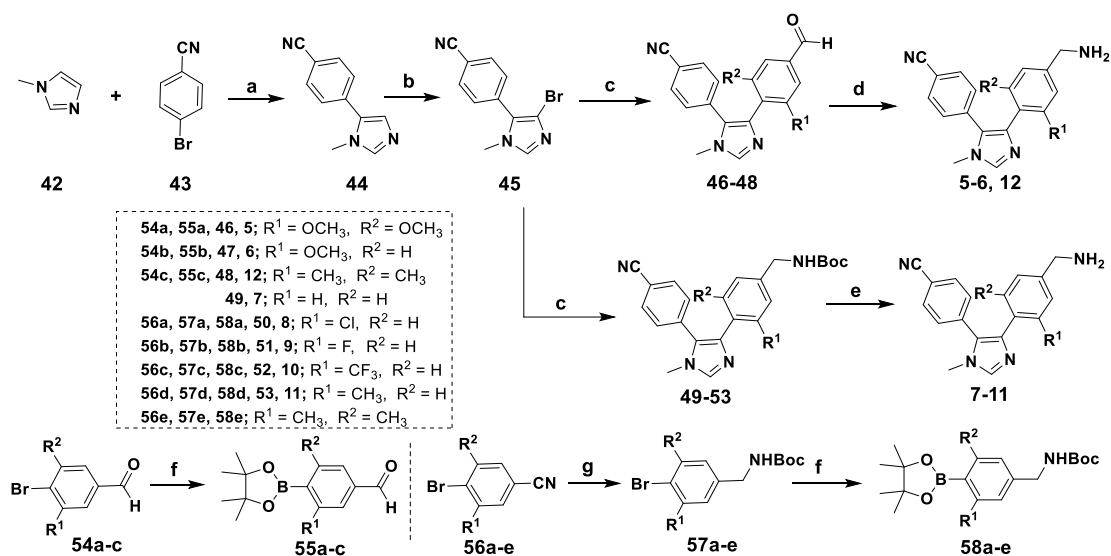
subjected to Suzuki coupling with boronic acid pinacol ester (**58e**), and the resulting **66a-b** were deprotected by HCl in dioxane to afford compounds **15** and **16**.

The general synthesis of compounds **17** – **20** was outlined in Scheme 4. The commercially available 5-bromo-1-methyl-1*H*-imidazole (**67**) was coupled with various boronic acids or boronic acid pinacol esters, and the resulting **68a-d** were treated with NBS to yield the intermediates **69a-d**. Another Suzuki coupling reaction was conducted between the intermediates **69a-d** and **58e**, followed by Boc-deprotection in TFA to obtain the target compounds **17** – **20**.

The general synthesis of compounds **21** – **27** was described in Scheme 5. The intermediate **61a** prepared in Scheme 2 was subjected to Suzuki coupling with appropriate boronic acid pinacol esters to produce the target compounds **21** – **23** and **26**. The compounds **22** and **23** were further reduced by NaBH₄ to yield compounds **24** and **25**, respectively. The target compound **27** was conveniently obtained from deprotection of compound **26**.

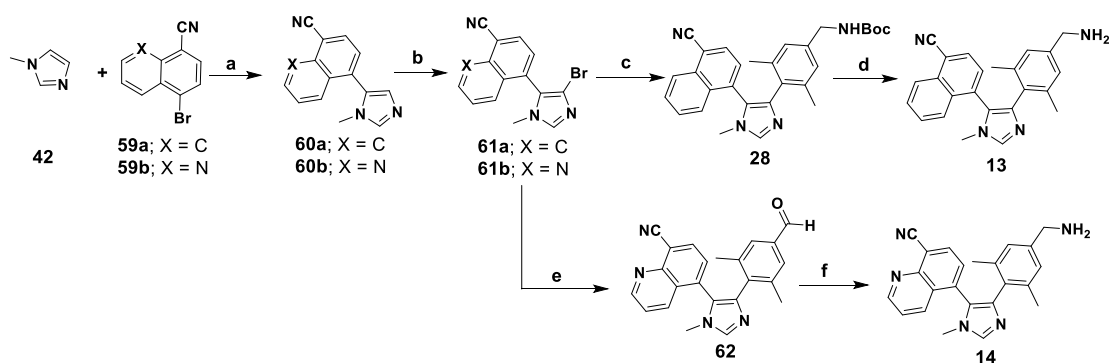
The general synthesis of compounds **29** – **41** was outlined in Scheme 6. The compound **22** bearing aldehyde group was subjected to reductive amination with various amines to afford the desired compounds **29** – **36**, **39** – **40** and **72**. Subsequently, the target compounds **37** – **38** and **41** were achieved by deprotection of Boc groups of compounds **35** – **36** and **72**.

Scheme 1. Synthesis of Compounds 5–12^a



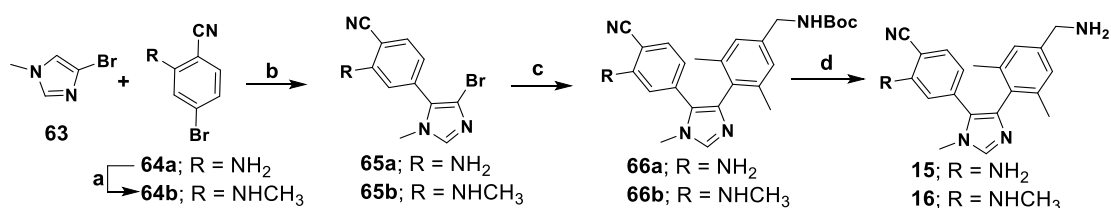
^aReagents and conditions: (a) Pd(OAc)₂, KOAc, DMAc, 120 °C, 10 h; (b) NBS, CH₃CN, 0 °C, 10 h; (c) **55a-c**, PdCl₂(dppf), K₂CO₃, dioxane/H₂O, 100 °C, 7 h; **58a-d**, XPhos Pd G2, K₃PO₄, dioxane/ H₂O, 90 °C, overnight; (d) CH₃COONH₄, CH₃COOH, NaBH₃CN, MeOH, 0 °C, 8 h; (e) trifluoroacetic acid, CH₂Cl₂, RT, 1 h; (f) Bis(pinacolato)diboron, PdCl₂(dppf), AcOK, dioxane, 80 °C, 8 h; and (g) for **57a-d**: BH₃/THF, THF, 0 °C to RT, overnight, and then (Boc)₂O, DIPEA, CH₂Cl₂, RT; for **57e**: (Boc)₂O, NiCl₂ 6H₂O, NaBH₄, MeOH, 0 °C, 4 h.

Scheme 2. Synthesis of Compounds 13-14 and 28^a



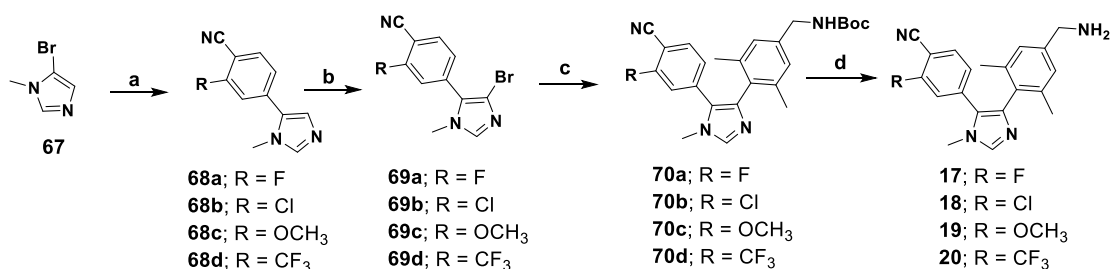
^aReagents and conditions: (a) Pd(OAc)₂, AcOK, DMAc, 120 °C, 10 h; (b) NBS, CH₃CN, 0 °C, 10 h; (c) **58e**, Pd(dppf)Cl₂, K₂CO₃, dioxane/H₂O, 85 °C, 24 h; (d) 4 M HCl in dioxane, RT, 1 h; (e) **55c**, Pd(amphos)Cl₂, Cs₂CO₃, dioxane/H₂O, 90 °C, 24 h; and (f) CH₃COONH₄, CH₃COOH, NaBH₃CN, MeOH, 0 °C, 8 h.

Scheme 3. Synthesis of Compounds 15 and 16^a



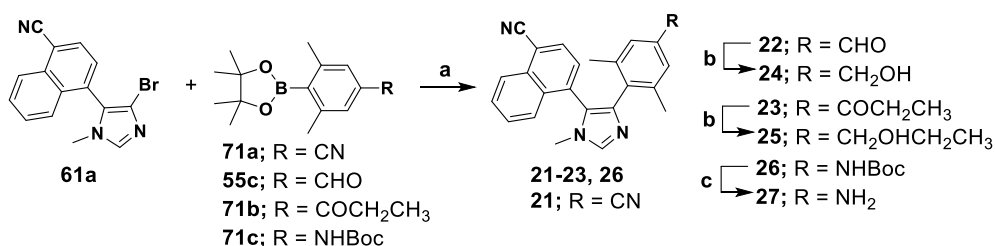
^aReagents and conditions: (a) MeI, K₂CO₃, DMF, RT, overnight; (b) Pd(OAc)₂, AcOK, DMAc, 120 °C, 18 h; (c) **58e**, Pd(amphos)Cl₂, Cs₂CO₃, dioxane/H₂O, 90°C, 24 h; and (d) 4 M HCl in dioxane, RT, 1 h.

Scheme 4. Synthesis of Compounds 17-20^a



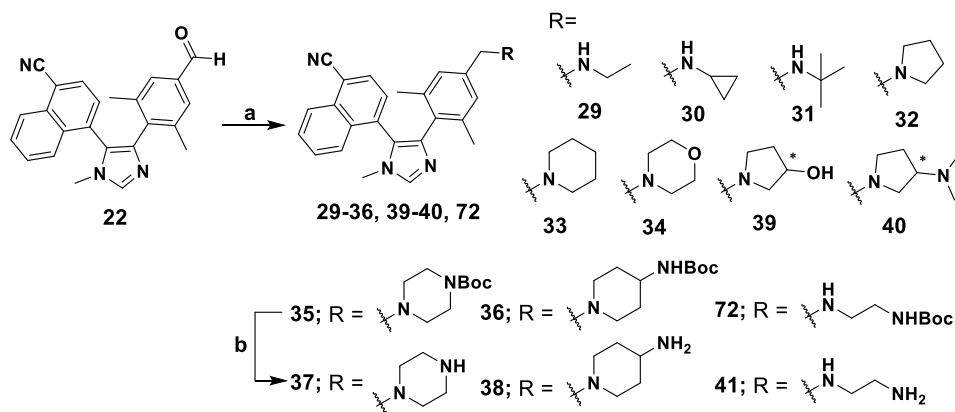
^aReagents and conditions: (a) appropriate boronic acid or boronic acid pinacol ester, Pd(dppf)Cl₂, Na₂CO₃, EtOH/H₂O/toluene, 100 °C, 10 h; (b) NBS, CH₃CN, -20 °C to RT, overnight; (c) XPhos Pd G2, K₃PO₄, dioxane/ H₂O, 100 °C, 10 h; and (d) trifluoroacetic acid, CH₂Cl₂, RT, 1 h.

Scheme 5. Synthesis of Compounds 21-27^a



^aReagents and conditions: (a) for **22** and **26**: Pd(amphos)Cl₂, Cs₂CO₃, dioxane/H₂O, 90 °C, 24 h; for **21** and **23**: Pd₂(dba)₃, PCy₃, K₃PO₄, toluene, 110°C, overnight; (b) NaBH₄, MeOH, RT, 5 h; and (c) 4 M HCl in dioxane, RT, 1 h.

Scheme 6. Synthesis of Compounds 29-41^a



^aReagents and conditions: (a) NaBH₃CN, MeOH, 0 °C, 5 h; and (b) 4 M HCl in dioxane, RT, 1 h.

CONCLUSIONS

Based on reported NSD3-PWWP1 inhibitor BI-9321 and NSD2-PWWP1 inhibitor MR837, we discovered a selective and *in vitro* effective NSD2-PWWP1 inhibitor **38** via rationally design and subsequent structure-based optimization. Compound **38** exhibited good potency against NSD2-PWWP1 (IC₅₀ = 0.11 ± 0.01 μM) and excellent selectivity over other PWWP domains. Finally, compound **38** was clarified as the most potent compound, which presented quite good enzyme inhibition activity and single digit micromole level of cell proliferation inhibition activity, after our unremitting efforts on optimizing the structure of the compounds.

EXPERIMENTAL SECTION

General Information. Unless otherwise noted, all starting materials, solvents and reagents were used directly as obtained commercially. All air and moisture sensitive reactions were carried out under an atmosphere of dry argon/nitrogen with heat-dried glassware and standard syringe techniques. ¹H NMR and ¹³C NMR spectra were recorded using CDCl₃ or CD₃OD on Varian Mercury-400, Bruker Advance 500 MHz or 600 MHz spectrometer with tetramethylsilane (TMS) as an internal standard. NMR

data are reported as follows: chemical shift, integration, multiplicity (s, singlet; d, doublet; t, triplet; m, multiplet; dd, doublet of doublets; brs, broad singlet), and coupling constants. Low-resolution ESI-MS was obtained with Thermo Fisher Finnigan LTQ or Finnigan LCQ Deca XP mass spectrometer using a CAPCELL PAK C18 (50 mm × 2.0 mm, 5 μm) or an Agilent ZORBAX Eclipse XDB C18 (50 mm × 2.1 mm, 5 μm) in positive or negative electrospray mode. High-resolution ESI-MS was recorded by using Finnigan MAT-95 mass spectrometer, Agilent G6520 Q-TOF mass spectrometer or Agilent G6230 TOF LC/MS spectrometer. The target compounds were analyzed for purity by high performance liquid chromatography (HPLC) and shown to have ≥95% purity. Purity of target compounds was determined on analytical Gilson-215 high performance liquid chromatography system using an YMC ODS3 column (50 mm × 4.6 mm, 5 μm), and conditions were as follows: CH₃CN/H₂O eluent at 2.5 mL/min flow [containing 0.1% trifluoroacetic acid (TFA)] at 35 °C, 8 min, gradient 5% CH₃CN to 95% CH₃CN, monitored by UV absorption at 214 and 254 nm. Purity of compounds **10** and **20** were determined by analytical Agilent-1290 high performance liquid chromatography using a Waters BEH C18 column (50 mm × 2.1 mm, 1.7 μm) and conditions were as follows: CH₃CN/H₂O eluent at 0.5 mL/min flow [containing 0.1% trifluoroacetic acid (TFA)] at 40 °C, 5 min, gradient 5% CH₃CN to 80% CH₃CN, monitored by UV absorption at 220 and 254 nm. All reactions were monitored by TLC analysis on silica gel GF254 plates and TLC spots were visualized under UV light. Column chromatography was carried out on silica gel (200-300 mesh) for routine purification.

Synthetic Procedures. The compound MR837 was prepared according to reported literature procedures for biological assay as positive control.¹²

4-(4-(4-(aminomethyl)-2,6-dimethoxyphenyl)-1-methyl-1H-imidazol-5-yl)benzotrile

(5). To a solution of 4-Bromobenzotrile **43** (3.00 g, 16.48 mmol) and 1-methyl-1H-imidazole **42** (2 mL, 32.96 mmol) in dimethylacetamide (25 mL) were added palladium acetate (370 mg, 1.65 mmol) and potassium acetate (3.24 g, 32.96 mmol). The reaction mixture was degassed with Ar₂ and stirred at 120 °C for 10 h. After cooling to rt, the reaction was quenched by addition of saturated aqueous NaCl (100 mL) and was extracted with EtOAc (3 × 20 mL). The combined organic phase was washed with brine (50 mL×5) and dried over anhydrous Na₂SO₄. The residue was purified by column chromatography on silica gel (4:1, 60 - 90 °C petroleum ether – EtOAc) to give the desired intermediate (**44**). Off-white solid (1.46 g, 48.3 %). ¹H NMR (400 MHz, Methanol-*d*₄) δ 7.82 – 7.77 (m, 2H), 7.76 (d, J = 1.1 Hz, 1H), 7.70 – 7.63 (m, 2H), 7.20 (d, J = 1.1 Hz, 1H), 3.77 (s, 3H).

To a solution of compound (**44**) (970 mg, 5.29 mmol) in CH₃CN (20 mL) under ice bath was added NBS (940 mg, 5.28 mmol) in three batches. The ice bath was removed and the mixture was stirred at rt for 10 h. The reaction was slowly quenched by saturated aqueous Na₂S₂O₃ and was extracted with EtOAc (3 × 10 mL). The combined organic phase was washed with brine (10 mL) and dried over anhydrous Na₂SO₄, filtered, and concentrated in vacuo. The residue was purified by column chromatography on silica gel (6:1, 60 - 90 °C petroleum ether – EtOAc) to give the intermediate (**45**). White solid (668 mg, 48.1 %). ¹H NMR (400 MHz, Methanol-*d*₄) δ

7.90 – 7.86 (m, 2H), 7.77 (s, 1H), 7.70 – 7.66 (m, 2H), 3.67 (s, 3H).

Compound **45** (145 mg, 554.53 μmol), **55a** (180 mg, 616.15 μmol), and K_2CO_3 (170 mg, 1.23 mmol) were dissolved in 1,4-dioxane (4.8 mL) and H_2O (1.2 mL). The mixture was degassed with Ar_2 and $\text{PdCl}_2(\text{dppf})$ (50 mg, 61.61 μmol) was added quickly under argon atmosphere. The reaction mixture was heated to 100 $^\circ\text{C}$ and stirred for 7 h. After completion of the reaction, the mixture was concentrated under reduced pressure and purified by column chromatography on silica gel (5:1, 60 - 90 $^\circ\text{C}$ petroleum ether – EtOAc) to give the intermediate (**46**). White solid (74 mg, 34.6 %). ^1H NMR (400 MHz, Methanol- d_4) δ 9.92 (d, $J = 0.9$ Hz, 1H), 7.85 (s, 1H), 7.71 – 7.65 (m, 2H), 7.44 – 7.38 (m, 2H), 7.17 (s, 2H), 3.74 (s, 3H), 3.67 (s, 6H).

To a solution of **46** (50 mg, 143.94 μmol) and ammonium acetate (111 mg, 1.44 mmol) in CH_3OH (4 mL) was added a drop of CH_3COOH and the resulting mixture was stirred at room temperature for 0.5 h. Sodium cyanoborohydride (46 mg, 215.91 μmol) was added into the mixture at 0 $^\circ\text{C}$ and the reaction mixture was then stirred for 8 h. Subsequently, the reaction was quenched by saturated aqueous NaHCO_3 , and was extracted with DCM - MeOH (5:1, 3 \times 5 mL). The combined organic phase was washed with brine (10 mL) and dried over anhydrous Na_2SO_4 , filtered, and concentrated in vacuo. The residue was purified by column chromatography on silica gel (20:1, DCM – MeOH) to obtain the desired product (**5**). Off-white amorphous solid (668 mg, 48.1 %). ^1H NMR (600 MHz, Methanol- d_4) δ 7.79 (s, 1H), 7.67 – 7.58 (m, 2H), 7.44 – 7.37 (m, 2H), 6.62 (s, 2H), 3.79 (s, 2H), 3.71 (s, 3H), 3.60 (s, 6H). ^{13}C NMR (151 MHz, Methanol- d_4) δ 160.54(*2C), 145.91, 140.02, 136.66, 134.28,

133.15(*2C), 130.92, 130.84(*2C), 119.56, 112.01, 111.43, 104.20(*2C), 56.04(*2C), 46.96, 33.26. HRMS (ESI): m/z $[M+H]^+$ $C_{20}H_{21}N_4O_2$ 349.1659; found 349.1661. HPLC: t_R = 2.000 min, 100%.

4-(4-(4-(aminomethyl)-2-methoxyphenyl)-1-methyl-1H-imidazol-5-yl)benzotrile

(**6**). The intermediate **47** was obtained from **45** through a procedure similar to the preparation of the intermediate **46**. Off-white solid. 71.4% yield. 1H NMR (400 MHz, Methanol- d_4) δ 9.93 (s, 1H), 7.88 (s, 1H), 7.75 (d, J = 0.6 Hz, 1H), 7.73 (d, J = 0.6 Hz, 1H), 7.71 – 7.66 (m, 1H), 7.54 (dd, J = 7.7, 1.5 Hz, 1H), 7.42 (d, J = 0.6 Hz, 1H), 7.40 (q, J = 1.5 Hz, 1H), 7.34 (d, J = 1.4 Hz, 1H), 3.71 (s, 3H), 3.33 (s, 3H).

The target compound **6** was prepared from **47** by following a similar method as described for compound **5**. Off-white amorphous solid. 52.3% yield. 1H NMR (600 MHz, Methanol- d_4) δ 7.81 (s, 1H), 7.72 – 7.69 (m, 2H), 7.41 – 7.38 (m, 2H), 7.36 (d, J = 7.7 Hz, 1H), 6.94 (d, J = 7.7 Hz, 1H), 6.88 (s, 1H), 3.79 (s, 2H), 3.70 (s, 3H), 3.34 (s, 3H). ^{13}C NMR (151 MHz, Methanol- d_4) δ 157.88, 144.88, 140.04, 137.64, 137.39, 133.25(*2C), 132.36, 131.16(*2C), 130.17, 122.98, 120.58, 119.55, 112.19, 111.36, 55.03, 46.54, 33.27. HRMS (ESI): m/z $[M + H]^+$ calcd for $C_{19}H_{19}N_4O$ 319.1553; found 319.1548. HPLC: t_R = 1.932 min, 96.54%.

4-(4-(4-(aminomethyl)-2,6-dimethylphenyl)-1-methyl-1H-imidazol-5-yl)benzotrile

(**12**). The intermediate **48** was obtained from **45** through a procedure similar to the preparation of the intermediate **46**. Orange solid. 12.4% yield. 1H NMR (400 MHz, Methanol- d_4) δ 9.91 (s, 1H), 7.98 (s, 1H), 7.68 (d, J = 8.3 Hz, 2H), 7.58 (s, 2H), 7.35 (dd, J = 7.4, 1.3 Hz, 2H), 3.81 (s, 3H), 2.09 (s, 6H).

The target compound **12** was prepared from **48** by following a similar method as described for compound **5**. Off-white amorphous solid. 58.3% yield. ¹H NMR (400 MHz, Methanol-*d*₄) δ 9.28 (s, 1H), 7.81 (d, J = 8.0 Hz, 2H), 7.56 (d, J = 8.1 Hz, 2H), 7.34 (s, 2H), 4.22 (s, 2H), 3.97 (s, 3H), 2.15 (s, 6H). ¹³C NMR (151 MHz, Methanol-*d*₄) δ 141.27(*2C), 138.47, 134.75, 134.05(*2C), 131.96, 131.74(*2C), 131.66, 131.34, 130.57(*2C), 127.37, 118.76, 115.00, 51.71, 35.43, 20.34(*2C). HRMS (ESI): *m/z* [M + H]⁺ calcd for C₂₀H₂₁N₄ 317.1761; found 317.1757. HPLC: *t*_R = 2.383 min, 96.77%.

4-(4-(4-(aminomethyl)phenyl)-1-methyl-1H-imidazol-5-yl)benzonitrile (7). Compound **45** (47.4 mg, 181 μmol), (4-(((tert-butoxycarbonyl)amino)methyl)phenyl)boronic acid (50 mg, 199 μmol), and K₃PO₄ (170 mg, 1.23 mmol) were dissolved in 1, 4-dioxane (4.8 mL) and H₂O (1.2 mL). The mixture was degassed with Ar₂ and XPhos Pd G2 (14.2 mg, 18.1 μmol) was added quickly under argon atmosphere. The reaction mixture was heated to 90 °C and stirred overnight. After completion of the reaction, the mixture was concentrated under reduced pressure and purified by column chromatography on silica gel (5:1, 60 - 90 °C petroleum ether – EtOAc) to give the intermediate (**49**) as a white solid. To a stirred solution of **49** in DCM (2 ml) at 0 °C was added TFA (1 ml) and the mixture stirred at rt for 1 h. The mixture was concentrated, and the residue was purified by column chromatography on silica gel (20:1, DCM – MeOH) to give compound **7**. White amorphous solid (12 mg, 23 % yield over two steps). ¹H NMR (600 MHz, Methanol-*d*₄) δ 7.82 – 7.81 (m, 2H), 7.80 (d, J = 1.9 Hz, 1H), 7.54 – 7.51 (m, 2H), 7.31 – 7.28 (m, 2H), 7.22 (d, J = 8.4 Hz, 2H),

3.75 (s, 2H), 3.61 (s, 3H). ^{13}C NMR (151 MHz, Methanol- d_4) δ 142.29, 140.23, 140.17, 136.50, 133.86(*2C), 133.79, 132.72(*2C), 130.88, 128.71(*2C), 128.56(*2C), 119.37, 113.32, 46.24, 32.92. HRMS (ESI): m/z $[\text{M} + \text{H}]^+$ calcd for $\text{C}_{18}\text{H}_{17}\text{N}_4$ 289.1448; found 289.1446. HPLC: $t_{\text{R}} = 1.854$ min, 96.01%.

4-(4-(4-(aminomethyl)-2-chlorophenyl)-1-methyl-1H-imidazol-5-yl)benzotrile (8).

The target compound **8** was prepared from **45** and **58a** by following a similar method as described for compound **7**. White amorphous solid (18 mg, 30 % yield over two steps). ^1H NMR (600 MHz, Methanol- d_4) δ 7.86 (s, 1H), 7.71 – 7.67 (m, 2H), 7.43 – 7.39 (m, 2H), 7.38 (d, $J = 1.4$ Hz, 1H), 7.33 (d, $J = 7.8$ Hz, 1H), 7.27 (dd, $J = 7.9, 1.7$ Hz, 1H), 3.78 (s, 2H), 3.74 (s, 3H). ^{13}C NMR (151 MHz, Methanol- d_4) δ 145.79, 140.32, 138.64, 135.92, 135.01, 133.70, 133.51(*2C), 132.85, 131.50(*2C), 130.61, 129.64, 127.01, 119.38, 112.70, 45.84, 33.34. HRMS (ESI): m/z $[\text{M} + \text{H}]^+$ calcd for $\text{C}_{18}\text{H}_{16}\text{ClN}_4$ 323.1058; found 307.1053. HPLC: $t_{\text{R}} = 2.233$ min, 100%.

4-(4-(4-(aminomethyl)-2-fluorophenyl)-1-methyl-1H-imidazol-5-yl)benzotrile (9).

The target compound **9** was prepared from **45** and **58b** by following a similar method as described for compound **7**. White amorphous solid (12 mg, 21 % yield over two steps). ^1H NMR (500 MHz, Methanol- d_4) δ 7.87 (s, 1H), 7.75 – 7.69 (m, 2H), 7.45 (dt, $J = 8.2, 1.6$ Hz, 2H), 7.41 (t, $J = 7.7$ Hz, 1H), 7.15 (dd, $J = 7.9, 1.6$ Hz, 1H), 7.01 (dd, $J = 11.2, 1.4$ Hz, 1H), 3.79 (s, 2H), 3.69 (s, 3H). ^{13}C NMR (126 MHz, Methanol- d_4) δ 140.64, 136.19, 133.52(*2C), 132.65, 132.62, 131.66(*2C), 130.88, 130.80, 130.73, 124.33, 119.41, 115.78, 115.60, 112.88, 45.82, 33.26. HRMS (ESI): m/z $[\text{M} + \text{H}]^+$ calcd for $\text{C}_{18}\text{H}_{16}\text{N}_4$ 307.1354; found 307.1352. HPLC: $t_{\text{R}} = 1.864$ min, 100%.

4-(4-(4-(aminomethyl)-2-(trifluoromethyl)phenyl)-1-methyl-1H-imidazol-5-yl)benzonitrile (10). The target compound **10** was prepared from **45** and **58c** by following a similar method as described for compound **7**. White amorphous solid (12 mg, 18 % yield over two steps). ¹H NMR (500 MHz, MeOD-*d*₄): δ 8.86 (s, 1H), 7.99 (d, *J* = 0.9 Hz, 1H), 7.79 (d, *J* = 8.5 Hz, 2H), 7.65 (d, *J* = 7.9 Hz, 1H), 7.55 (d, *J* = 8.5 Hz, 2H), 4.27 (s, 2H), 3.86 (s, 3H). LRMS (ESI): *m/z* [M+H]⁺ calcd for C₁₉H₁₆F₃N₄ 357.1; found 357.3. HPLC: *t*_R = 3.814 min, 99.01%.

4-(4-(4-(aminomethyl)-2-methylphenyl)-1-methyl-1H-imidazol-5-yl)benzonitrile (11). The target compound **11** was prepared from **45** and **58d** by following a similar method as described for compound **7**. White amorphous solid (17 mg, 32 % yield over two steps). ¹H NMR (600 MHz, Methanol-*d*₄) δ 7.85 (s, 1H), 7.67 (d, *J* = 8.3 Hz, 2H), 7.42 – 7.32 (m, 2H), 7.17 (s, 1H), 7.10 (s, 2H), 3.74 (s, 2H), 3.74 (s, 3H), 2.05 (s, 3H). ¹³C NMR (151 MHz, Methanol-*d*₄) δ 143.43, 141.07, 140.27, 138.57, 136.06, 133.48(*2C), 132.19, 131.56(*2C), 130.39, 129.77, 125.75, 119.40, 112.43, 46.32, 33.37, 20.22. HRMS (ESI): *m/z* [M + H]⁺ calcd for C₁₉H₁₉N₄ 303.1604; found 303.1609. HPLC: *t*_R = 1.917 min, 95.59%.

tert-butyl

(4-(5-(4-cyanonaphthalen-1-yl)-1-methyl-1H-imidazol-4-yl)-3,5-dimethylbenzyl)carbamate (28). The intermediate **60a** was obtained from **42** and **59a** through a procedure similar to the preparation of the intermediate **44**. Light green amorphous solid. 63.4 % yield. ¹H NMR (400 MHz, Methanol-*d*₄) δ 8.32 – 8.25 (m, 1H), 8.10 (d, *J* = 7.4 Hz, 1H), 7.90 (d, *J* = 1.1 Hz, 1H), 7.84 – 7.78 (m, 2H), 7.71 (ddd, *J* = 8.0, 6.9, 1.3 Hz, 1H),

7.64 (d, $J = 7.4$ Hz, 1H), 7.16 (d, $J = 1.2$ Hz, 1H), 3.49 (s, 3H).

The intermediate **61a** was obtained from **60a** through a procedure similar to the preparation of the intermediate **45**. White solid. 32.4 % yield. ^1H NMR (400 MHz, Methanol- d_4) δ 8.32 (dt, $J = 8.4, 1.0$ Hz, 1H), 8.15 (d, $J = 7.4$ Hz, 1H), 7.89 (s, 1H), 7.84 (ddd, $J = 8.3, 6.9, 1.3$ Hz, 1H), 7.73 (ddd, $J = 8.2, 6.8, 1.2$ Hz, 1H), 7.67 (d, $J = 7.4$ Hz, 1H), 7.64 (dt, $J = 8.5, 1.0$ Hz, 1H), 3.46 (s, 3H).

The target compound **28** was prepared from **61a** and **58e** by following a similar method as described for compound **46**. Yellow amorphous solid (21 mg, 14.2 % yield). ^1H NMR (400 MHz, Chloroform- d) δ 8.28 (d, $J = 8.2$ Hz, 1H), 7.81 (s, 1H), 7.80 (d, $J = 7.4$ Hz, 1H), 7.76 – 7.67 (m, 2H), 7.66 – 7.56 (m, 1H), 7.24 (d, $J = 7.4$ Hz, 1H), 6.90 (s, 1H), 6.70 (s, 1H), 4.14 (d, $J = 5.2$ Hz, 2H), 3.43 (s, 3H), 2.22 (s, 3H), 1.79 (s, 3H), 1.42 (s, 9H). HRMS (ESI): m/z $[\text{M} + \text{H}]^+$ calcd for $\text{C}_{29}\text{H}_{31}\text{N}_4\text{O}_2$ 467.2442; found 467.2437. HPLC: $t_R = 3.205$ min, 100%.

4-(4-(4-(aminomethyl)-2,6-dimethylphenyl)-1-methyl-1H-imidazol-5-yl)-1-naphtho nitrile (13). The compound **28** (10 mg, 21.4 μmol) was dissolved in 4 M HCl in 1,4-dioxane solution (2 mL) at room temperature and stirred for 1 h. The solvent was removed in vacuo, neutralized with ammonia alcohol solution and purified by column chromatography on silica gel (20:1, DCM – MeOH) to obtain the desired product (**13**). Yellow amorphous solid (6 mg, 82.3 %). ^1H NMR (400 MHz, Methanol- d_4) δ 9.40 (s, 1H), 8.30 (d, $J = 8.2$ Hz, 1H), 8.05 (d, $J = 6.7$ Hz, 1H), 7.95 (d, $J = 7.3$ Hz, 1H), 7.91 – 7.79 (m, 2H), 7.65 (d, $J = 6.8$ Hz, 1H), 7.26 (s, 1H), 7.10 (s, 1H), 4.01 (s, 2H), 3.73 (s, 3H), 2.35 (s, 3H), 2.05 (s, 3H). ^{13}C NMR (151 MHz, Methanol- d_4) δ 141.63, 141.10,

138.58, 136.82, 133.67, 133.28, 132.82, 131.18, 131.04, 130.96, 130.88, 130.67, 129.44, 129.35, 129.27, 127.26, 126.91(*2C), 117.60, 114.22, 43.69, 35.56, 20.80, 20.72. ESI ($[M+H]^+$) m/z : 367.27. HRMS (ESI): m/z $[M + H]^+$ calcd for $C_{24}H_{23}N_4$ 367.1917; found 367.1910. HPLC: t_R = 2.268 min, 97.79%.

5-(4-(4-(aminomethyl)-2,6-dimethylphenyl)-1-methyl-1H-imidazol-5-yl)quinoline-8-carbonitrile (14). The intermediate **60b** was obtained from **42** and **59b** through a procedure similar to the preparation of the intermediate **60a**. Light brown solid. 42.5 % yield. 1H NMR (400 MHz, Chloroform-*d*) δ 9.21 – 9.10 (m, 1H), 8.32 – 8.12 (m, 2H), 7.72 (s, 1H), 7.64 – 7.50 (m, 2H), 7.23 (s, 1H), 3.52 (s, 3H).

The intermediate **61b** was obtained from **60b** through a procedure similar to the preparation of the intermediate **61a**. Light yellow solid. 89.1 % yield. 1H NMR (400 MHz, Chloroform-*d*) δ 9.17 (d, J = 3.9 Hz, 1H), 8.24 (d, J = 7.3 Hz, 2H), 8.01 (d, J = 8.3 Hz, 1H), 7.73 – 7.52 (m, 2H), 3.47 (s, 3H).

Compound **61b** (77 mg, 294.7 μ mol), **55c** (92 mg, 294.7 μ mol), and CS_2CO_3 (288 mg, 884.1 μ mol) were dissolved in 1, 4-dioxane (4.8 mL) and H_2O (1.2 mL). The mixture was degassed with Ar_2 and $Pd(amphos)Cl_2$ (21 mg, 29.47 μ mol) was added quickly under argon atmosphere. The reaction mixture was heated to 90 $^\circ C$ and stirred for 24 h. After completion of the reaction, the mixture was concentrated under reduced pressure and purified by column chromatography on silica gel (4:1, 60 - 90 $^\circ C$ petroleum ether – EtOAc) to give the intermediate **62**. Light yellow solid (20 mg, 22.4%). 1H NMR (400 MHz, Chloroform-*d*) δ 9.85 (s, 1H), 9.11 (dd, J = 4.1, 1.4 Hz, 1H), 8.05 (d, J = 7.4 Hz, 1H), 8.03 – 7.98 (m, 1H), 7.90 (s, 1H), 7.53 (dd, J = 8.5, 4.2

Hz, 1H), 7.48 (s, 1H), 7.38 (s, 1H), 7.34 (d, $J = 7.5$ Hz, 1H), 3.51 (s, 3H), 2.22 (s, 3H), 1.97 (s, 3H).

The target compound **14** was prepared from **62** by following a similar method as described for compound **5**. Light yellow amorphous solid (8 mg, 42.0%). ^1H NMR (500 MHz, Methanol- d_4) δ 9.10 – 9.05 (m, 2H), 8.32 (ddd, $J = 8.5, 4.4, 1.4$ Hz, 1H), 8.26 (d, $J = 7.5$ Hz, 1H), 7.79 – 7.68 (m, 2H), 7.21 (d, $J = 14.2$ Hz, 1H), 7.11 (d, $J = 17.5$ Hz, 1H), 3.99 (s, 2H), 3.71 (s, 3H), 2.26 (s, 3H), 2.06 (s, 3H). ^{13}C NMR (126 MHz, Methanol- d_4) δ 154.33, 148.39, 141.41, 140.76, 139.41, 136.50, 136.27, 135.47, 131.40, 131.36, 130.72, 130.11, 129.32, 129.26, 128.70, 125.24, 125.21, 117.23, 116.16, 43.72, 34.97, 20.71, 20.68. HRMS (ESI): m/z $[\text{M} + \text{H}]^+$ calcd for $\text{C}_{23}\text{H}_{22}\text{N}_5$ 368.1870; found 322.1872. HPLC: $t_{\text{R}} = 2.712$ min, 100%.

2-amino-4-(4-(4-(aminomethyl)-2,6-dimethylphenyl)-1-methyl-1H-imidazol-5-yl)benzonitrile (15). To a solution of 2-amino-4-bromobenzonitrile **64a** (500 mg, 2.54 mmol) and 4-bromo-1-methyl-1H-imidazole **42** (310 μL , 3.05 mmol) in dimethylacetamide (10 mL) were added palladium acetate (60 mg, 254 μmol) and potassium acetate (500 mg, 5.10 mmol). The reaction mixture was degassed with Ar_2 and stirred at 120 $^\circ\text{C}$ for 18 h. After cooling to rt, the reaction was quenched by addition of saturated aqueous NaCl (40 mL) and was extracted with EtOAc (3 \times 20 mL). The combined organic phase was washed with brine (20 mL \times 5) and dried over anhydrous Na_2SO_4 . The residue was purified by column chromatography on silica gel (2:1, 60 - 90 $^\circ\text{C}$ petroleum ether – EtOAc) to give the desired intermediate **65a**. Off-white solid (191 mg, 27.2 %). ^1H NMR (400 MHz, Chloroform- d) δ 7.48 (d, $J =$

8.3 Hz, 2H), 6.81 (d, $J = 1.5$ Hz, 1H), 6.74 (dd, $J = 8.0, 1.5$ Hz, 1H), 4.60 (s, 2H), 3.60 (s, 3H).

The intermediate **66a** was obtained from **65a** and **58e** through a procedure similar to the preparation of the intermediate **62**. Light brown solid. 8.2% yield. ^1H NMR (400 MHz, Chloroform- d) δ 7.68 (s, 1H), 7.29 (d, $J = 8.1$ Hz, 1H), 6.89 (s, 2H), 6.46 (d, $J = 8.1$ Hz, 1H), 6.38 (s, 1H), 4.41 (s, 2H), 4.22 (d, $J = 5.9$ Hz, 2H), 3.70 (s, 3H), 1.97 (s, 6H), 1.46 (s, 9H).

The compound **66a** (20 mg, 46.3 μmol) was dissolved in 4 M HCl in 1, 4-dioxane solution (4 mL) at room temperature and stirred for 1 h. The solvent was removed in vacuo to obtain the desired product **15** as a hydrochloride salt. Yellow amorphous solid (16 mg, 96%). ^1H NMR (400 MHz, Methanol- d_4) δ 9.11 (s, 1H), 7.37 (d, $J = 8.0$ Hz, 1H), 7.25 (s, 2H), 6.76 (d, $J = 1.5$ Hz, 1H), 6.54 (dd, $J = 8.0, 1.5$ Hz, 1H), 4.08 (s, 2H), 3.91 (s, 3H), 2.16 (s, 6H). ^{13}C NMR (126 MHz, Methanol- d_4) δ 152.99, 141.24, 137.93, 136.75, 134.42, 132.74, 132.40, 130.88, 130.79, 129.32, 127.26, 122.83, 118.08, 117.80, 117.16, 97.06, 43.82, 35.36, 20.38(*2C). HRMS (ESI): m/z $[\text{M} + \text{H}]^+$ calcd for $\text{C}_{20}\text{H}_{22}\text{N}_5$ 322.1870; found 322.1866. HPLC: $t_{\text{R}} = 1.922$ min, 100%.

4-(4-(4-(aminomethyl)-2,6-dimethylphenyl)-1-methyl-1H-imidazol-5-yl)-2-(methylamino)benzotrile (16). To a mixture of 2-amino-4-bromobenzotrile (**64a**, 300 mg, 1.52 mmol) and K_2CO_3 (421 mg, 3.05 mmol) in *N, N*-dimethylformamide (10 mL) was added CH_3I (105 μL , 1.67 mmol) at room temperature. The resulting mixture was stirred overnight before quenched by 2 M NaOH aqueous solution and was extracted with EtOAc (3 \times 20 mL). The combined organic phase was washed with brine (20

mL×5) and dried over anhydrous Na₂SO₄, filtered, and concentrated under reduced pressure. The residue was purified by column chromatography on silica gel (3:1, 60 - 90 °C petroleum ether – EtOAc) to give the desired intermediate **64b**. White solid. (148 mg, 46.0 %).

The intermediate **65b** was obtained from **63** and **64b** through a procedure similar to the preparation of the intermediate **65a**. White solid. 34.1% yield. ¹H NMR (400 MHz, Chloroform-*d*) δ 7.44 (d, *J* = 7.9 Hz, 2H), 6.68 (d, *J* = 1.4 Hz, 1H), 6.65 (dd, *J* = 7.9, 1.4 Hz, 1H), 4.86 (s, 1H), 3.60 (s, 3H), 2.94 (s, 3H).

The intermediate **66b** was obtained from **65b** and **58e** through a procedure similar to the preparation of the intermediate **62**. White solid. 7.8% yield. ¹H NMR (400 MHz, Chloroform-*d*) δ 7.69 (s, 1H), 7.32 (d, *J* = 8.0 Hz, 1H), 6.91 (s, 2H), 6.49 (dd, *J* = 8.0, 1.5 Hz, 1H), 6.21 (s, 1H), 4.54 (d, *J* = 5.2 Hz, 1H), 4.22 (d, *J* = 5.8 Hz, 2H), 3.76 (s, 3H), 2.57 (d, *J* = 4.9 Hz, 3H), 1.99 (s, 6H), 1.46 (s, 9H).

The target compound **16** was prepared from **66b** by following a similar method as described for compound **15**. Light yellow amorphous solid (6 mg, 86.5%). ¹H NMR (400 MHz, Methanol-*d*₄) δ 9.06 (s, 1H), 7.43 (d, *J* = 7.9 Hz, 1H), 7.26 (s, 2H), 6.64 – 6.59 (m, 1H), 6.55 (s, 1H), 4.09 (s, 2H), 3.94 (s, 3H), 2.70 (s, 3H), 2.16 (s, 6H). ¹³C NMR (151 MHz, Methanol-*d*₄) δ 152.83, 141.26(*2C), 138.11, 136.65, 134.88, 133.06, 133.01, 132.88, 130.88, 129.28(*2C), 117.86, 117.34, 112.38, 97.44, 43.81, 35.38, 29.91, 20.36(*2C). HRMS (ESI): *m/z* [M + H]⁺ calcd for C₂₁H₂₄N₅ 346.2026; found 346.2036. HPLC: *t*_R = 2.073 min, 100%.

4-(4-(4-(aminomethyl)-2,6-dimethylphenyl)-1-methyl-1H-imidazol-5-yl)-2-fluorobenzamide

nzonitrile (17). (4-cyano-3-fluorophenyl)boronic acid (1.48 g, 9.0 mmol) and 5-bromo-1-methyl-1H-imidazole (**67**, 966 mg, 6.0 mmol) was suspended in EtOH/H₂O/toluene (30 mL/ 3 mL/ 6 mL), followed by addition of Na₂CO₃ (2.83 g, 27.0 mmol) and Pd(dppf)Cl₂ (200 mg, 0.3 mmol) under argon atmosphere. The mixture was stirred at 100 °C for 10 h and was then concentrated and purified by column chromatography on silica gel (4:1, 60 - 90 °C petroleum ether – EtOAc) to afford the intermediate **68a**. Yellow solid (900 mg, 75% yield). ¹H NMR (500 MHz, Chloroform-*d*) δ 7.69 (dd, *J* = 6.5, 8.0 Hz, 1H), 7.59 (s, 1H), 7.32 (dd, *J* = 1.5, 7.0 Hz, 1H), 7.28-7.26 (m, 2H), 3.67 (s, 3H).

To a stirred solution of intermediate **68a** (201 mg, 1.0 mmol) in MeCN (20 ml) was added NBS (201 mg, 1.0 mmol, 1.0 equiv) at -20 °C. The mixture was slowly warmed to room temperature and stirred overnight. The reaction was slowly quenched by saturated aqueous Na₂S₂O₃ and was extracted with EtOAc (3 × 10 mL). The combined organic phase was washed with brine (10 mL) and dried over anhydrous Na₂SO₄, filtered, and concentrated in vacuo. The residue was purified by column chromatography on silica gel (5:1, 60 - 90 °C petroleum ether – EtOAc) to give the intermediate **69a**. White solid (150 mg, 54% yield). ¹H NMR (500 MHz, Chloroform-*d*) δ 7.76-7.73 (m, 1H), 7.52 (s, 1H), 7.36-7.31 (m, 2H), 3.66 (s, 3H).

The target compound **17** was prepared from **69a** and **58e** by following a similar method as described for compound **7**. White amorphous solid (5 mg, 7.5% yield over two steps). ¹H NMR (600 MHz, Methanol-*d*₄) δ 9.30 (s, 1H), 7.86 (s, 1H), 7.42 – 7.35 (m, 2H), 7.29 (s, 2H), 4.10 (s, 2H), 3.99 (s, 3H), 2.16 (s, 6H). ¹³C NMR (151 MHz,

Methanol- d_4) δ 164.93, 163.21, 141.21(*2C), 138.82, 137.21, 135.92, 134.09 (d, J = 8.4 Hz), 130.85 (d, J = 42.6 Hz), 129.60(*2C), 128.03, 127.08, 119.01 (d, J = 21.5 Hz), 113.81, 103.94 (d, J = 15.2 Hz), 43.84, 36.22, 20.57(*2C). HRMS (ESI): m/z [$M + H$]⁺ calcd for C₂₀H₂₀FN₄ 335.1667; found 335.1664. HPLC: t_R = 2.054 min, 100%.

4-(4-(4-(aminomethyl)-2,6-dimethylphenyl)-1-methyl-1H-imidazol-5-yl)-2-chlorobenzonitrile (18). The intermediate **68b** was obtained from **67** through a procedure similar to the preparation of the intermediate **68a**. Yellow solid (500 mg, 90% yield). ¹H NMR (500 MHz, Chloroform- d) δ 7.73 (d, J = 8.5 Hz, 1H), 7.60 (brs, 1H), 7.55 (d, J = 2.0 Hz, 1H), 7.32 (dd, J = 1.5, 9.5 Hz, 1H), 7.28 (brs, 1H), 3.75 (s, 3H).

The intermediate **69b** was obtained from **68b** through a procedure similar to the preparation of the intermediate **69a**. Yellow solid (436 mg, 64% yield). ¹H NMR (500 MHz, MeOD- d_4) δ 7.97 (d, J = 8.5 Hz, 1H), 7.84-7.81 (m, 2H), 7.65 (dd, J = 1.5, 9.5 Hz, 1H), 3.72 (s, 3H).

The target compound **18** was prepared from **69b** and **58e** by following a similar method as described for compound **7**. White amorphous solid (6 mg, 8.6% yield over two steps). ¹H NMR (500 MHz, MeOD- d_4): δ 8.84 (s, 1H), 7.85 (d, J = 8.0 Hz, 1H), 7.59 (s, 1H), 7.43 (d, J = 8.0 Hz, 1H), 7.25 (s, 2H), 4.10 (s, 2H), 3.92 (s, 3H), 1.31 (s, 6H). HRMS (ESI): m/z [$M + H$]⁺ calcd for C₂₀H₂₀ClN₄ 351.1371; found 351.1372. HPLC: t_R = 2.083 min, 100%.

4-(4-(4-(aminomethyl)-2,6-dimethylphenyl)-1-methyl-1H-imidazol-5-yl)-2-methoxybenzonitrile (19). The intermediate **68c** was obtained from **67** through a procedure similar to the preparation of the intermediate **68a**. Yellow amorphous solid (640 mg,

56% yield). ^1H NMR (500 MHz, Chloroform-*d*) δ 7.62 (d, $J = 8.5$ Hz, 1H), 7.57 (brs, 1H), 7.22 (brs, 1H), 7.02 (dd, $J = 1.5, 8.5$ Hz, 1H), 6.97 (d, $J = 1.5$ Hz, 1H), 3.97 (s, 3H), 3.72 (s, 3H).

The intermediate **69c** was obtained from **68c** through a procedure similar to the preparation of the intermediate **69a**. Yellow solid (240 mg, 82% yield). ^1H NMR (500 MHz, Chloroform-*d*) δ 7.66 (d, $J = 8.0$ Hz, 1H), 7.50 (s, 1H), 7.08 (d, $J = 1.5$ Hz, 1H), 7.03 (dd, $J = 1.5, 8.0$ Hz, 1H), 3.96 (s, 3H), 3.64 (s, 3H).

The target compound **19** was prepared from **69c** and **58e** by following a similar method as described for compound **7**. White amorphous solid (8 mg, 11.6% yield over two steps). ^1H NMR (600 MHz, Methanol-*d*₄) δ 9.26 (s, 1H), 7.67 (d, $J = 7.9$ Hz, 1H), 7.29 (s, 2H), 7.13 (s, 1H), 7.05 (d, $J = 7.8$ Hz, 1H), 4.10 (s, 2H), 4.00 (s, 3H), 3.84 (s, 3H), 2.17 (s, 6H). ^{13}C NMR (151 MHz, Methanol-*d*₄) δ 162.65, 141.29, 138.16, 137.10, 135.59(*2C), 133.14, 132.23, 130.17, 129.47(*2C), 127.54, 123.18, 116.18, 114.20, 104.16, 57.23, 43.75, 35.79, 20.38(*2C). HRMS (ESI): m/z [M + H]⁺ calcd for C₂₁H₂₃N₄O 347.1866; found 347.1863. HPLC: $t_R = 2.083$ min, 100%.

4-(4-(4-(aminomethyl)-2,6-dimethylphenyl)-1-methyl-1H-imidazol-5-yl)-2-(trifluoromethoxy)benzotrile (20). The intermediate **68d** was obtained from **67** through a procedure similar to the preparation of the intermediate **68a**. Yellow solid (850 mg, 44% yield). ^1H NMR (500 MHz, Chloroform-*d*) δ 7.91 (d, $J = 8.0$ Hz, 1H), 7.82 (s, 1H), 7.71 (dd, $J = 1.5, 8.0$ Hz, 1H), 7.67-7.61 (m, 2H), 3.77 (s, 3H).

The intermediate **69d** was obtained from **68d** through a procedure similar to the preparation of the intermediate **69a**. Yellow solid (670 mg, 57% yield). ^1H NMR (500

MHz, Chloroform-*d*) δ 7.97 (d, $J = 8.0$ Hz, 1H), 7.87 (s, 1H), 7.78 (dd, $J = 1.5, 8.0$ Hz, 1H), 7.55 (s, 1H), 3.67 (s, 3H).

The target compound **20** was prepared from **69d** and **58e** by following a similar method as described for compound **7**. White amorphous solid (12 mg, 15.6% yield over two steps). ^1H NMR (500 MHz, MeOD-*d*₄): δ 9.06 (s, 1H), 8.08 (d, $J = 8.0$ Hz, 1H), 7.88 (s, 1H), 7.81 (dd, $J = 1.5, 8.0$ Hz, 1H), 7.26 (s, 2H), 4.10 (s, 2H), 3.96 (s, 3H), 2.145 (s, 6H). HRMS (ESI): m/z $[\text{M} + \text{H}]^+$ calcd for C₂₁H₂₀F₃N₄ 385.1605; found 385.0275. HPLC: $t_{\text{R}} = 4.211$ min, 95.31%.

4-(4-(4-cyano-2,6-dimethylphenyl)-1-methyl-1H-imidazol-5-yl)-1-naphthonitrile (**21**). Compound **61a** (100 mg, 321.36 μmol), **71a** (99 mg, 385.63 μmol), tricyclohexylphosphane (9 mg, 32.14 μmol) and K₃PO₄ (137 mg, 642.71 μmol) were suspended in toluene (5 mL). The mixture was degassed with Ar₂ and Pd₂(dba)₃ (30 mg, 32.14 μmol) was added quickly under argon atmosphere. The reaction mixture was heated to 110 °C and stirred overnight. After completion of the reaction, the mixture was concentrated under reduced pressure and purified by column chromatography on silica gel (2:1, 60 - 90 °C petroleum ether – EtOAc) to give the desired compound **21**. Yellow amorphous solid (15 mg, 12.9%). ^1H NMR (500 MHz, Chloroform-*d*) δ 8.31 (d, $J = 8.4$ Hz, 1H), 7.85 (s, 1H), 7.82 (d, $J = 7.4$ Hz, 1H), 7.73 (ddd, $J = 8.2, 6.8, 1.2$ Hz, 1H), 7.69 (d, $J = 8.1$ Hz, 1H), 7.63 (ddd, $J = 8.3, 6.7, 1.1$ Hz, 1H), 7.30 (s, 1H), 7.21 (d, $J = 7.4$ Hz, 1H), 7.11 (s, 1H), 3.46 (s, 3H), 2.26 (s, 3H), 1.86 (s, 3H). ^{13}C NMR (126 MHz, Chloroform-*d*) δ 139.54, 138.81, 138.78, 138.05, 137.86, 132.27, 131.90, 131.45, 131.09, 130.21, 130.19, 128.49, 127.99, 127.61,

127.05, 125.73, 125.32, 118.47, 116.72, 111.09, 110.94, 32.37, 20.27, 20.02. HRMS (ESI): m/z $[M + H]^+$ calcd for $C_{24}H_{19}N_4$ 363.1604; found 363.1603. HPLC: t_R = 2.912 min, 96.04%.

4-(4-(4-formyl-2,6-dimethylphenyl)-1-methyl-1H-imidazol-5-yl)-1-naphthonitrile (**22**). The target compound **22** was prepared from **61a** and **55c** by following a similar method as described for compound **62**. Yellow amorphous solid (21 mg, 18.3% yield). Purity > 90%. 1H NMR (400 MHz, Chloroform-*d*) δ 9.85 (s, 1H), 8.36 – 8.26 (m, 1H), 7.84 (s, 1H), 7.80 (d, J = 7.4 Hz, 1H), 7.76 – 7.70 (m, 2H), 7.66 – 7.60 (m, 1H), 7.52 (d, J = 1.5 Hz, 1H), 7.33 (s, 1H), 7.22 (d, J = 7.4 Hz, 1H), 3.47 (s, 4H), 2.32 (s, 3H), 1.90 (s, 3H). ^{13}C NMR (151 MHz, Chloroform-*d*) δ 192.65, 139.91, 139.86, 139.31, 139.11, 139.03, 135.68, 132.87, 132.64, 132.09, 131.73, 129.06, 128.79, 128.57(*2C), 128.29, 127.57, 126.30, 126.04, 117.40, 111.57, 33.04, 21.02, 20.76. HRMS (ESI): m/z $[M + H]^+$ calcd for $C_{24}H_{20}N_3O$ 366.1601; found 366.1594. HPLC: t_R = 2.892 min, 95.40%.

4-(4-(2,6-dimethyl-4-propionylphenyl)-1-methyl-1H-imidazol-5-yl)-1-naphthonitril e (**23**). The target compound **23** was prepared from **61a** and **71b** by following a similar method as described for compound **21**. Yellow amorphous solid (41 mg, 32.8% yield). 1H NMR (400 MHz, Chloroform-*d*) δ 8.33 – 8.25 (m, 1H), 7.91 (s, 1H), 7.79 (d, J = 7.4 Hz, 1H), 7.75 – 7.68 (m, 2H), 7.67 – 7.60 (m, 1H), 7.59 (d, J = 1.8 Hz, 1H), 7.40 (d, J = 1.8 Hz, 1H), 7.22 (d, J = 7.4 Hz, 1H), 3.47 (s, 3H), 2.89 (q, J = 7.2 Hz, 2H), 2.29 (s, 3H), 1.87 (s, 3H), 1.15 (t, J = 7.2 Hz, 3H). LRMS (ESI): m/z $[M+H]^+$ calcd for $C_{26}H_{24}N_3O$ 394.19; found 394.33.

4-(4-(4-(hydroxymethyl)-2,6-dimethylphenyl)-1-methyl-1H-imidazol-5-yl)-1-naphth
onitrile (24). To a solution of compound **22** (20 mg, 54.73 μmol) in anhydrous
 CH_3OH (3 mL) was added NaBH_4 (4 mg, 109.46 μmol), and the resulting mixture
was stirred at room temperature for 5 h. Then, the reaction was quenched by saturated
aqueous NaCl , and the resulting mixture was extracted with $\text{DCM} - \text{CH}_3\text{OH}$ (10:1, 3
 \times 50 mL). The combined organic phase was dried over anhydrous Na_2SO_4 , filtered,
and concentrated under reduced pressure. The residue was purified by column
chromatography on silica gel (30:1, $\text{DCM} - \text{MeOH}$) to give the compound **24**.
Off-white amorphous solid (15 mg, 74.6 %). ^1H NMR (400 MHz, $\text{Methanol-}d_4$) δ
9.35 (s, 1H), 8.30 (d, $J = 8.1$ Hz, 1H), 8.03 (d, $J = 7.4$ Hz, 1H), 7.93 (d, $J = 8.2$ Hz,
1H), 7.86 (t, $J = 7.2$ Hz, 1H), 7.82 – 7.77 (m, 1H), 7.61 (d, $J = 7.4$ Hz, 1H), 7.12 (s,
1H), 6.95 (s, 1H), 4.47 (s, 2H), 3.71 (s, 3H), 2.30 (s, 3H), 1.97 (s, 3H). ^{13}C NMR (151
MHz, $\text{Methanol-}d_4$) δ 145.41, 140.42, 139.89, 138.16, 133.73, 133.28, 132.81, 132.05,
130.95, 130.86, 130.78, 130.53, 129.40, 127.31, 127.24, 126.97, 126.82, 125.10,
117.67, 114.22, 64.39, 35.40, 20.70, 20.64. HRMS (ESI): m/z $[\text{M} + \text{H}]^+$ calcd for
 $\text{C}_{24}\text{H}_{22}\text{N}_3\text{O}$ 368.1757; found 368.1758. HPLC: $t_{\text{R}} = 2.647$ min, 100%.

4-(4-(4-(1-hydroxypropyl)-2,6-dimethylphenyl)-1-methyl-1H-imidazol-5-yl)-1-naph
thonitrile (25). The target compound **25** was prepared from **23** by following a similar
method as described for compound **24**. Light yellow amorphous solid (13 mg, 66.7%
yield). ^1H NMR (600 MHz, $\text{Methanol-}d_4$) δ 8.23 (d, $J = 8.3$ Hz, 1H), 8.04 (s, 1H),
7.92 (d, $J = 7.4$ Hz, 1H), 7.80 (d, $J = 8.4$ Hz, 1H), 7.79 – 7.75 (m, 1H), 7.71 – 7.67 (m,
1H), 7.41 (dd, $J = 7.4, 4.5$ Hz, 1H), 6.97 (d, $J = 29.5$ Hz, 1H), 6.82 (d, $J = 30.5$ Hz,

1H), 4.34 (q, J = 6.9 Hz, 1H), 3.51 (s, 3H), 2.21 (d, J = 2.6 Hz, 3H), 1.88 (d, J = 4.7 Hz, 3H), 1.64 (ddq, J = 33.8, 12.7, 7.1 Hz, 2H), 0.79 (t, J = 7.4 Hz, 3H). ¹³C NMR (151 MHz, Methanol-d₄) δ 144.56, 138.93, 138.89, 138.27 (d, J = 19.9 Hz), 137.58 (d, J = 27.3 Hz), 132.87, 132.41, 131.87, 131.82, 131.67, 128.74, 128.38, 128.09 (d, J = 4.1 Hz), 127.36, 126.24, 125.13, 125.00, 124.36 (d, J = 9.2 Hz), 116.77, 110.62, 74.97, 31.75, 31.28, 19.67, 19.50, 9.06. HRMS (ESI): *m/z* [M + H]⁺ calcd for C₂₆H₂₆N₃O 396.2070; found 396.2071. HPLC: *t_R* = 2.839 min, 98.09%.

tert-butyl

(4-(5-(4-cyanonaphthalen-1-yl)-1-methyl-1H-imidazol-4-yl)-3,5-dimethylphenyl)carbamate (26). The target compound **26** was prepared from **61a** and **71b** by following a similar method as described for compound **62**. White amorphous solid (25 mg, 9.2% yield). ¹H NMR (600 MHz, Chloroform-*d*) δ 8.27 (d, J = 8.3 Hz, 1H), 7.79 (d, J = 7.5 Hz, 2H), 7.73 – 7.66 (m, 2H), 7.62 – 7.57 (m, 1H), 7.23 (d, J = 7.4 Hz, 1H), 7.03 (s, 1H), 6.78 (s, 1H), 6.51 – 6.45 (m, 1H), 3.42 (s, 3H), 2.19 (s, 3H), 1.77 (s, 3H), 1.46 (s, 9H). ¹³C NMR (151 MHz, Chloroform-*d*) δ 152.84, 140.00, 139.47, 138.80, 138.76, 137.65, 133.38, 132.79, 132.17, 131.91, 128.80, 128.37, 128.25, 128.20, 127.46, 126.27, 126.07, 117.59, 117.04, 117.01, 110.97, 80.35, 32.87, 28.42(*3C), 21.10, 20.83. HRMS (ESI): *m/z* [M + H]⁺ calcd for C₂₈H₂₉N₄O₂ 453.2285; found 453.2288. HPLC: *t_R* = 3.310 min, 95.75%.

4-(4-(4-amino-2,6-dimethylphenyl)-1-methyl-1H-imidazol-5-yl)-1-naphthonitrile (27).

The target compound **27** was prepared from **26** by following a similar method as described for compound **13**. White amorphous solid (10 mg, 85% yield). ¹H NMR

(500 MHz, Methanol- d_4) δ 9.43 (s, 1H), 8.30 (d, $J = 8.1$ Hz, 1H), 8.06 (d, $J = 7.4$ Hz, 1H), 7.95 (d, $J = 8.3$ Hz, 1H), 7.89 – 7.85 (m, 1H), 7.82 (ddd, $J = 8.1, 7.1, 1.2$ Hz, 1H), 7.66 (d, $J = 7.4$ Hz, 1H), 7.21 (d, $J = 1.9$ Hz, 1H), 7.04 (d, $J = 1.8$ Hz, 1H), 3.74 (s, 3H), 2.37 (s, 3H), 2.07 (s, 3H). ^{13}C NMR (126 MHz, Methanol- d_4) δ 143.39, 142.82, 138.74, 134.18, 133.71, 133.32, 132.73, 131.36, 130.91, 130.89, 130.70, 130.27, 128.99, 127.16, 126.97, 126.76, 123.39, 123.31, 117.62, 114.38, 35.51, 20.79, 20.72. HRMS (ESI): m/z $[\text{M} + \text{H}]^+$ calcd for $\text{C}_{23}\text{H}_{21}\text{N}_4$ 353.1761; found 353.1760. HPLC: $t_{\text{R}} = 2.285$ min, 98.88%.

4-(4-(4-((ethylamino)methyl)-2,6-dimethylphenyl)-1-methyl-1H-imidazol-5-yl)-1-naphthonitrile (29). To a solution of **22** (50 mg, 136.8 μmol) in CH_3OH (4 mL) was added and ethylamine aqueous solution (0.5 mL) and the resulting mixture was stirred at $^\circ\text{C}$ for 1 h. Sodium cyanoborohydride (17 mg, 273.6 μmol) was added into the mixture and the reaction mixture was then stirred at 0 $^\circ\text{C}$ for 5 h. Subsequently, the reaction was quenched by saturated aqueous NaHCO_3 , and was extracted with DCM - MeOH (5:1, 3 \times 5 mL). The combined organic phase was washed with brine (10 mL) and dried over anhydrous Na_2SO_4 , filtered, and concentrated in vacuo. The residue was purified by column chromatography on silica gel (20:1, DCM – MeOH) to obtain the desired product **29**. White amorphous solid (14 mg, 26.7 %). ^1H NMR (400 MHz, Methanol- d_4) δ 9.39 (s, 1H), 8.30 (d, $J = 8.2$ Hz, 1H), 8.05 (d, $J = 7.4$ Hz, 1H), 7.95 (d, $J = 8.2$ Hz, 1H), 7.87 (t, $J = 7.2$ Hz, 1H), 7.84 – 7.77 (m, 1H), 7.65 (d, $J = 7.4$ Hz, 1H), 7.31 (s, 1H), 7.16 (s, 1H), 4.07 (s, 2H), 3.73 (s, 3H), 3.05 (q, $J = 7.3$ Hz, 2H), 2.34 (s, 3H), 2.06 (s, 3H), 1.29 (t, $J = 7.3$ Hz, 3H). ^{13}C NMR (151 MHz, Methanol- d_4) δ

141.68, 141.16, 138.56, 135.10, 133.67, 133.28, 132.80, 131.18, 131.03, 130.91, 130.87, 130.63, 130.32, 130.23, 129.30, 127.74, 126.90, 126.85, 117.62, 114.20, 51.28, 44.05, 35.43, 20.72, 20.66, 11.42. HRMS (ESI): m/z $[M + H]^+$ calcd for $C_{26}H_{27}N_4$ 395.2230; found 395.2239. HPLC: $t_R = 2.373$ min, 100%.

The target compounds **30** – **36**, **39** – **40** and **72** were prepared from **22** by following a similar method as described for compound **29**. Subsequently, the target compounds **37** – **38** and **41** were prepared from **37** – **38** and **72** by following a similar method as described for compound **13**.

4-(4-(4-((cyclopropylamino)methyl)-2,6-dimethylphenyl)-1-methyl-1H-imidazol-5-yl)-1-naphthonitrile (30). White amorphous solid (25 mg, 44.9 %). 1H NMR (400 MHz, Methanol- d_4) δ 9.42 (s, 1H), 8.29 (d, $J = 8.2$ Hz, 1H), 8.05 (d, $J = 7.4$ Hz, 1H), 7.95 (d, $J = 8.2$ Hz, 1H), 7.86 (t, $J = 7.4$ Hz, 1H), 7.83 – 7.78 (m, 1H), 7.65 (d, $J = 7.4$ Hz, 1H), 7.32 (s, 1H), 7.17 (s, 1H), 4.20 (s, 2H), 3.74 (s, 3H), 2.71 (p, $J = 5.5$ Hz, 1H), 2.34 (s, 3H), 2.06 (s, 3H), 0.84 (d, $J = 5.4$ Hz, 4H). ^{13}C NMR (151 MHz, Methanol- d_4) δ 141.66, 141.12, 138.55, 134.87, 133.66, 133.27, 132.78, 131.06, 131.01, 130.95, 130.87, 130.65, 130.54, 130.45, 129.21, 127.62, 126.89, 126.86, 117.60, 114.22, 52.32, 35.52, 31.28, 20.73, 20.66, 4.19(*2C). HRMS (ESI): m/z $[M + H]^+$ calcd for $C_{27}H_{27}N_4$ 407.2230; found 407.2235. HPLC: $t_R = 2.394$ min, 100%.

4-(4-(4-((tert-butylamino)methyl)-2,6-dimethylphenyl)-1-methyl-1H-imidazol-5-yl)-1-naphthonitrile (31). White amorphous solid (27 mg, 47.6 %). 1H NMR (500 MHz, Methanol- d_4) δ 8.23 (d, $J = 8.3$ Hz, 1H), 8.04 (s, 1H), 7.91 (d, $J = 7.4$ Hz, 1H), 7.83 – 7.73 (m, 2H), 7.69 (ddd, $J = 8.3, 7.0, 1.2$ Hz, 1H), 7.41 (d, $J = 7.4$ Hz, 1H), 7.02 (s,

1H), 6.86 (s, 1H), 3.61 (s, 2H), 3.51 (s, 3H), 2.22 (s, 3H), 1.90 (s, 3H), 1.17 (s, 9H).
¹³C NMR (126 MHz, Methanol-*d*₄) δ 139.00, 138.75, 138.67, 138.13, 132.89, 132.39, 132.10, 131.88, 131.85(*2C), 128.80, 128.41, 128.14(*2C), 127.41, 127.38, 126.23, 125.12, 116.73, 110.64, 51.72, 45.85, 31.72, 26.67(*3C), 19.53, 19.41. HRMS (ESI): *m/z* [M + H]⁺ calcd for C₂₈H₃₁N₄ 423.2543; found 423.2544. HPLC: *t*_R = 2.488 min, 97.20%.

4-(4-(2,6-dimethyl-4-(pyrrolidin-1-ylmethyl)phenyl)-1-methyl-1H-imidazol-5-yl)-1-naphthonitrile (32). White amorphous solid (25 mg, 44.3 %). ¹H NMR (600 MHz, Methanol-*d*₄) δ 8.21 (d, *J* = 8.3 Hz, 1H), 8.04 (s, 1H), 7.91 (d, *J* = 7.4 Hz, 1H), 7.79 (d, *J* = 8.4 Hz, 1H), 7.74 (t, *J* = 7.5 Hz, 1H), 7.67 (t, *J* = 7.6 Hz, 1H), 7.41 (d, *J* = 7.4 Hz, 1H), 6.98 (s, 1H), 6.83 (s, 1H), 3.51 (s, 3H), 3.45 (s, 2H), 2.44 (s, 4H), 2.18 (s, 3H), 1.90 (s, 3H), 1.74 (s, 4H). ¹³C NMR (151 MHz, Methanol-*d*₄) δ 140.43, 140.17, 139.81, 139.16, 138.95, 134.26, 133.80, 133.42, 133.27, 133.15, 130.12, 129.75, 129.44, 129.37(*2C), 128.79, 127.65, 126.51, 118.16, 111.99, 61.11, 54.85(*2C), 33.16, 23.99(*2C), 20.94, 20.85. HRMS (ESI): *m/z* [M + H]⁺ calcd for C₂₈H₂₉N₄ 421.2387; found 421.2388. HPLC: *t*_R = 2.379 min, 96.07%.

4-(4-(2,6-dimethyl-4-(piperidin-1-ylmethyl)phenyl)-1-methyl-1H-imidazol-5-yl)-1-naphthonitrile (33). White amorphous solid (25 mg, 42.1 %). ¹H NMR (600 MHz, Methanol-*d*₄) δ 8.22 (d, *J* = 8.3 Hz, 1H), 8.04 (s, 1H), 7.92 (d, *J* = 7.4 Hz, 1H), 7.79 (d, *J* = 8.4 Hz, 1H), 7.75 (ddd, *J* = 8.2, 7.0, 1.1 Hz, 1H), 7.67 (ddd, *J* = 8.2, 7.0, 1.1 Hz, 1H), 7.41 (d, *J* = 7.4 Hz, 1H), 6.96 (s, 1H), 6.82 (s, 1H), 3.52 (s, 3H), 3.32 (s, 2H), 2.17 (s, 3H), 1.90 (s, 3H), 1.53 (p, *J* = 5.6 Hz, 4H), 1.20 – 1.18 (m, 6H). ¹³C NMR

(151 MHz, Methanol- d_4) δ 139.05, 138.79, 138.28, 137.64, 136.28, 132.86, 132.42, 132.08, 131.87, 131.74, 129.48, 128.72, 128.57, 128.34, 128.02, 127.40, 126.26, 125.11, 116.77, 110.60, 74.43, 62.97(*2C), 31.77, 24.87(*2C), 23.63(*2C), 19.52. HRMS (ESI): m/z $[M + H]^+$ calcd for $C_{29}H_{31}N_4$ 435.2543; found 435.2549. HPLC: t_R = 2.440 min, 100%.

4-(4-(2,6-dimethyl-4-(morpholinomethyl)phenyl)-1-methyl-1H-imidazol-5-yl)-1-naphthonitrile (34). White amorphous solid (30 mg, 50.5 %). 1H NMR (400 MHz, Methanol- d_4) δ 9.39 (s, 1H), 8.30 (d, J = 8.2 Hz, 1H), 8.06 (d, J = 7.4 Hz, 1H), 7.94 (d, J = 8.2 Hz, 1H), 7.86 (t, J = 7.4 Hz, 1H), 7.85 – 7.77 (m, 1H), 7.65 (d, J = 7.4 Hz, 1H), 7.40 (s, 1H), 7.25 (s, 1H), 4.26 (s, 2H), 3.98 (d, J = 11.4 Hz, 2H), 3.78 (d, J = 10.8 Hz, 2H), 3.73 (s, 3H), 3.25 (s, 2H), 3.16 (d, J = 11.5 Hz, 2H), 2.35 (s, 3H), 2.06 (s, 3H). ^{13}C NMR (126 MHz, Methanol- d_4) δ 141.83, 141.29, 138.66, 133.72, 133.36, 132.74, 132.04, 131.98, 131.91, 131.09, 131.01, 130.91, 130.85, 130.62, 129.23, 128.53, 126.94, 126.82, 117.64, 114.28, 64.77(*2C), 61.18, 52.94(*2C), 35.44, 20.71, 20.68. HRMS (ESI): m/z $[M + H]^+$ calcd for $C_{28}H_{29}N_4O$ 437.2336; found 437.2339. HPLC: t_R = 2.394 min, 99.07%.

tert-butyl

4-(4-(5-(4-cyanonaphthalen-1-yl)-1-methyl-1H-imidazol-4-yl)-3,5-dimethylbenzyl)piperazine-1-carboxylate (35). White amorphous solid (30 mg, 40.9%). 1H NMR (400 MHz, Chloroform- d) δ 8.27 (dd, J = 8.3, 1.4 Hz, 1H), 7.88 (s, 1H), 7.79 (d, J = 7.4 Hz, 1H), 7.73 – 7.65 (m, 2H), 7.60 (ddd, J = 8.4, 7.0, 1.3 Hz, 1H), 7.25 (d, J = 7.4 Hz, 1H), 6.95 – 6.90 (m, 1H), 6.74 (d, J = 1.7 Hz, 1H), 3.43 (s, 3H), 3.39 (m, 4H), 3.35 (s, 2H),

2.35 – 2.30 (m, 4H), 2.20 (s, 3H), 1.81 (s, 3H), 1.43 (s, 9H). ¹³C NMR (151 MHz, Chloroform-*d*) δ 174.65, 154.84, 139.70, 138.98, 138.47, 137.83, 136.47, 133.13, 132.79, 132.09, 131.86, 128.84, 128.38(*2C), 128.32, 128.28, 127.32, 126.25, 126.07, 117.52, 111.15, 79.71, 62.73(*2C), 52.78, 32.96, 28.51(*3C), 20.92, 20.71. HRMS (ESI): *m/z* [M + H]⁺ calcd for C₃₃H₃₈N₅O₂ 536.3020; found 536.3015. HPLC: *t_R* = 2.699 min, 98.48%.

tert-butyl

(1-(4-(5-(4-cyanonaphthalen-1-yl)-1-methyl-1H-imidazol-4-yl)-3,5-dimethylbenzyl)piperidin-4-yl)carbamate (**36**). White amorphous solid (34 mg, 45.1%). ¹H NMR (600 MHz, Chloroform-*d*) δ 8.27 (d, *J* = 8.3 Hz, 1H), 7.82 – 7.76 (m, 2H), 7.75 – 7.67 (m, 2H), 7.62 – 7.57 (m, 1H), 7.25 (d, *J* = 8.0 Hz, 1H), 6.92 (s, 1H), 6.74 (s, 1H), 4.47 – 4.37 (m, 1H), 3.43 (s, 3H), 3.31 (s, 2H), 2.79 – 2.65 (m, 2H), 2.27 – 2.14 (m, 4H), 2.06 – 1.96 (m, 4H), 1.86 (d, *J* = 11.3 Hz, 2H), 1.82 (s, 3H), 1.43 (s, 9H). ¹³C NMR (151 MHz, Chloroform-*d*) δ 175.39, 155.11, 140.13, 138.70, 138.21, 137.55, 133.26, 132.63, 131.93, 131.71, 129.94, 129.66, 128.61, 128.11, 128.06, 128.03, 127.07, 126.16, 125.88, 117.41, 110.82, 79.13, 62.79, 52.29, 35.83, 32.69, 28.34(*3C), 25.45, 22.60, 20.76, 20.53, 14.04. HRMS (ESI): *m/z* [M + H]⁺ calcd for C₃₄H₄₀N₅O₂ 550.3177; found 550.3170. HPLC: *t_R* = 2.680 min, 100%.

4-(4-(2,6-dimethyl-4-(piperazin-1-ylmethyl)phenyl)-1-methyl-1H-imidazol-5-yl)-1-naphthonitrile (**37**). White amorphous solid (10 mg, 85%). ¹H NMR (400 MHz, Methanol-*d*₄) δ 9.42 (s, 1H), 8.30 (d, *J* = 8.1 Hz, 1H), 8.07 (d, *J* = 7.3 Hz, 1H), 7.95 (d, *J* = 8.2 Hz, 1H), 7.87 (t, *J* = 7.2 Hz, 1H), 7.85 – 7.79 (m, 1H), 7.65 (d, *J* = 7.4 Hz, 1H),

7.47 (s, 1H), 7.31 (s, 1H), 4.40 (s, 2H), 3.72 (s, 3H), 3.65 – 3.49 (m, 8H), 2.37 (s, 3H), 2.05 (s, 3H). ¹³C NMR (151 MHz, Methanol-*d*₄) δ 141.96, 141.40, 138.60, 133.71, 133.44, 132.74, 132.10, 131.98, 131.75, 131.12, 130.96, 130.86, 130.77, 130.68, 129.08, 128.52, 126.97, 126.80, 117.66, 114.32, 60.84, 49.28(*2C), 41.85(*2C), 35.46, 20.71, 20.66. HRMS (ESI): *m/z* [M + H]⁺ calcd for C₂₈H₃₀N₅ 436.2496; found 436.2499. HPLC: *t*_R = 2.225 min, 97.66%.

4-(4-(4-((4-aminopiperidin-1-yl)methyl)-2,6-dimethylphenyl)-1-methyl-1H-imidazol-5-yl)-1-naphthonitrile (38). White amorphous solid (11 mg, 88%). ¹H NMR (600 MHz, Methanol-*d*₄) δ 8.21 (d, *J* = 8.3 Hz, 1H), 8.04 (s, 1H), 7.90 (dd, *J* = 8.6, 4.4 Hz, 1H), 7.79 (d, *J* = 8.4 Hz, 1H), 7.76 – 7.72 (m, 1H), 7.68 – 7.63 (m, 1H), 7.41 (d, *J* = 7.4 Hz, 1H), 6.95 (s, 1H), 6.81 (s, 1H), 3.52 (s, 3H), 3.31 (s, 2H), 2.77 – 2.70 (m, 2H), 2.56 (dt, *J* = 10.7, 6.6 Hz, 1H), 2.17 (s, 3H), 1.95 (t, *J* = 11.6 Hz, 2H), 1.90 (s, 3H), 1.76 – 1.72 (m, 2H), 1.38 – 1.29 (m, 2H). ¹³C NMR (126 MHz, Methanol-*d*₄) δ 141.79, 141.24, 138.66, 133.66, 133.43, 132.69, 132.43, 131.97, 131.88, 131.04, 131.01, 130.88, 130.83, 130.63, 129.16, 128.33, 126.87(*2C), 117.66, 114.18, 60.82, 51.70(*2C), 46.82, 35.64, 28.24(*2C), 20.74(*2C). HRMS (ESI): *m/z* [M + H]⁺ calcd for C₂₉H₃₂N₅ 450.2652; found 450.2656. HPLC: *t*_R = 2.199 min, 99.25%.

4-(4-(4-((3-hydroxypyrrolidin-1-yl)methyl)-2,6-dimethylphenyl)-1-methyl-1H-imidazol-5-yl)-1-naphthonitrile (39). White amorphous solid (22 mg, 37.2%). ¹H NMR (400 MHz, Methanol-*d*₄) δ 8.23 (d, *J* = 8.3 Hz, 1H), 8.04 (s, 1H), 7.93 (d, *J* = 7.4 Hz, 1H), 7.78 (q, *J* = 8.0, 7.4 Hz, 2H), 7.71 – 7.64 (m, 1H), 7.41 (d, *J* = 7.4 Hz, 1H), 6.99 (s, 1H), 6.84 (s, 1H), 4.28 (tt, *J* = 6.9, 3.3 Hz, 1H), 3.52 (s, 3H), 3.50 – 3.41 (m, 2H),

2.71 (dt, J = 10.6, 5.5 Hz, 1H), 2.63 (q, J = 7.7 Hz, 1H), 2.46 (q, J = 8.5 Hz, 1H), 2.37 (dd, J = 10.4, 3.2 Hz, 1H), 2.19 (s, 3H), 2.08 (dd, J = 13.6, 7.3 Hz, 1H), 1.88 (s, 3H), 1.70 – 1.59 (m, 1H). ¹³C NMR (126 MHz, Methanol-*d*₄) δ 140.42, 140.20, 139.83, 139.16, 138.94, 134.27, 133.83, 133.39, 133.28, 133.17, 130.13, 129.75, 129.45, 129.23, 128.81, 127.65, 126.53, 118.18, 112.02, 71.42, 63.31, 61.22, 53.68, 49.51, 35.06, 33.15(*2C), 20.92. HRMS (ESI): *m/z* [M + H]⁺ calcd for C₂₈H₂₉N₄O 437.2336; found 437.2338. HPLC: *t*_R = 2.343 min, 100%.

4-(4-(4-((3-(dimethylamino)pyrrolidin-1-yl)methyl)-2,6-dimethylphenyl)-1-methyl-1H-imidazol-5-yl)-1-naphthonitrile (40). White amorphous solid (20 mg, 31.2%). ¹H NMR (500 MHz, Methanol-*d*₄) δ 9.40 (s, 1H), 8.31 (d, J = 8.2 Hz, 1H), 8.07 (d, J = 7.2 Hz, 1H), 7.93 (d, J = 8.2 Hz, 1H), 7.87 (t, J = 7.5 Hz, 1H), 7.82 (t, J = 7.4 Hz, 1H), 7.65 (d, J = 7.2 Hz, 1H), 7.44 (s, 1H), 7.28 (s, 1H), 4.43 (s, 2H), 4.23 (s, 1H), 3.88 – 3.82 (m, 1H), 3.78 (s, 1H), 3.73 (s, 3H), 3.57 (s, 1H), 3.43 (s, 1H), 2.95 (s, 6H), 2.60 (s, 1H), 2.43 (s, 1H), 2.35 (s, 3H), 2.05 (s, 3H). ¹³C NMR (126 MHz, Methanol-*d*₄) δ 141.97, 141.41, 138.61, 133.72, 133.51, 133.40, 132.74, 131.15, 131.12, 131.04, 130.95, 130.92, 130.87, 130.67, 129.13, 128.32, 126.97, 126.80, 117.65, 114.31, 64.61, 58.93, 54.22, 42.76, 35.50(*2C), 26.90, 23.70, 20.68(*2C). HRMS (ESI): *m/z* [M + H]⁺ calcd for C₃₀H₃₄N₅ 464.2809; found 464.2811. HPLC: *t*_R = 2.279 min, 100%.

4-(4-(4-(((2-aminoethyl)amino)methyl)-2,6-dimethylphenyl)-1-methyl-1H-imidazol-5-yl)-1-naphthonitrile (41). White amorphous solid (10 mg, 80%). ¹H NMR (500 MHz, Methanol-*d*₄) δ 9.40 (s, 1H), 8.30 (d, J = 8.3 Hz, 1H), 8.05 (d, J = 7.0 Hz, 1H),

7.93 (d, J = 8.2 Hz, 1H), 7.87 (t, J = 7.5 Hz, 1H), 7.81 (t, J = 7.4 Hz, 1H), 7.63 (d, J = 7.2 Hz, 1H), 7.40 (s, 1H), 7.24 (s, 1H), 4.19 (s, 2H), 3.72 (s, 3H), 3.41 (t, J = 6.6 Hz, 2H), 3.34 (t, J = 6.3 Hz, 2H), 2.35 (s, 3H), 2.04 (s, 3H). ¹³C NMR (126 MHz, Methanol-*d*₄) δ 141.74, 141.20, 138.57, 134.60, 133.69, 133.34, 132.80, 131.10, 131.03, 130.96, 130.90, 130.69, 130.54, 130.41, 129.15, 127.79, 126.95, 126.83, 117.61, 114.30, 52.09, 45.66, 36.80, 35.52, 20.74, 20.67. HRMS (ESI): *m/z* [M + H]⁺ calcd for C₂₆H₂₈N₅ 410.2339; found 410.2337. HPLC: *t*_R = 2.172 min, 100%.

Protein Expression and Purification. DNA fragment encoding amino acids 211 to 350 of NSD2-PWWP1 subcloned in the pET-28 plasmid was produced by Shanghai Generay Biotech Co. Ltd. The constructed plasmid containing six histidine or sumo tags in the N-terminus was transformed into *Escherichia coli* BL21(DE3) cell with heat shock. Transformed *E. coli* cells were grown to an OD₆₀₀ of 1.2–1.5 at 37 °C in TB medium containing 50 mg/L kanamycin. Then, the culture temperature was reduced to 18 °C and the cultures were then induced with 0.5 mM IPTG for 16 h. The bacterial cells were harvested after centrifugation, washed with PBS for 3 times and frozen at -80 °C. Harvested bacterial cells were lysed with ultra-high pressure cell disrupter (UH-03, Union, Shanghai, China) in lysis buffer (50 mM Tris, pH 8.0, 50 mM NaCl, 5% glycerol, and 0.5 mM TCEP). The supernatant was collected after centrifugation at 12000 rpm for 60min. Subsequently, Ni Sepherose was added to the supernatant to bind to the protein, and the target protein was eluted with a buffer containing 250 mM imidazole. The target protein was concentrated and purified with exclusion chromatography (Superdex 200 10/300 GL124mL) which was balanced by

buffer (50 mM HEPES, 50 mM NaCl, 5% glycerol, pH 8.0 and 0.5 mM TCEP). Purified NSD2-PWWP1 protein concentrated to 10mg/ml with approximately 95% purity was either used to set up crystals or flash frozen in liquid nitrogen for storage at -78 °C.

Crystallization and X-ray Crystallography. The vapor diffusion method was used for crystallization of aliquots of the purified proteins. The protein of NSD2-PWWP1, and the ligands were grown at 16 °C in 1 µL of protein with an equal volume of reservoir solution containing the 1.6 M ammonium sulfate, 0.01 M magnesium chloride, 0.1 M HEPES at pH 7.5. Crystals grew to diffracting quality within 1 week. Data was collected at 100 K on beam line BL17U at the Shanghai Synchrotron Radiation Facility (SSRF) (Shanghai, China) for the co-crystallized structures.¹⁶ The data were processed with the XDS software packages¹⁷, and the structures were then solved by molecular replacement using the PHENIX software package.¹⁸ The search model used for the crystals was the NSD2-PWWP1 complex structure (PDB code 6UE6). The structures were refined using the CCP4 program REFMAC5¹⁹ combined with the simulated annealing protocol implemented in the program PHENIX. With the aid of the program Coot²⁰, compound, water molecules, and others were fitted into the initial F_o-F_c maps.

Enzymatic Assays for NSD2-PWWP1. The enzyme activity was determined by HTRF assay which was conducted according to the manufacturer's protocol (Cisbio) in a 96-well plate. First, 5 µL of 4 nM NSD2 PWWP1 diluent buffer and 5 µL of the substrate substrate polypeptide diluent buffer was added to each well, then 5 µL of the

corresponding concentration of compounds dissolved in diluent buffer, finally, 5 μ L of Tb/d2 mixture were then added. After incubated at room temperature for 3 h, the plate was read on a microplate reader (BioTek Cytation 5) at 665 and 620 nm. HTRF signals were calculated as a ratio as follows: (intensity of 665 nm)/(intensity of 620 nm) $\times 10^4$. All compounds were dissolved in DMSO and added to the medium at a final 1:1000 dilution. All experiments were repeated at least twice. The enzyme activity calculation formula was as follows: Inhibition= (maximum intensity for complete binding of protein and peptide- intensity after adding the inhibitor)/(maximum intensity for complete binding of protein and peptide- background values of intensity only containing Tb and d2) $\times 100\%$. The calculation of compounds IC₅₀ took the logarithm of compound concentration as the abscissa, and the corresponding inhibition ratio as the ordinate, and nonlinear fitting was performed. The reagents and equipment used in this experiment were as follows: the fluorescent donor was Anti-His Tb (Cisbio,PerkinElmer), the fluorescent receptor was Streptavidin-d2, the protein was His-NSD2-PWWP1(211-350aa) purified in our laboratory, and the substrate polypeptide was Biotin-ATKAARKSAPATGGV-Lys (me)₂-KPHRYRPG (Shanghai Desheng Pharmaceutical Technology Co., Ltd), buffer used from Cisbio Perkinelmer.

Thermal Shift Assay. Melting curves of proteins with and without the presence of compounds were determined by TSA using the Protein thermal shift™ Dye Kit (Life Technologies). The kit containing Protein Thermal Shift™ Buffer and Protein Thermal Shift™ Dye. The reaction system contained 5ul Protein Thermal Shift™

Buffer, 2.5ul Diluted Protein Thermal Shift™ Dye (8X) and 12.5ul Water + protein + buffer and/or buffer components. The melting curve was generated by heating the plate with a slope of 2.5 °C/min from 25 °C to 95 °C. The assay was performed on QuantStudio™ 6 Flex real-time PCR machine (Applied Biosystems) and analyzed by the software Protein Thermal Shift™v1.3 (Applied Biosystems).

AlphaLISA NSD2 Histone H3 Lysine-N-methyltransferase Assay. AlphaLISA NSD2 Histone H3 Lysine-N-methyltransferase assay were used to determined the IC₅₀ of compound **9c**. The enzyme prep was diluted in assay buffer before use. SAM (TAKA) was used as the methyl group donor and unmethylated histone H3 (Anaspec) was used as a substrate. All these components were incubated at room temperature (r.t.) for 20 min. Add 5 µL of high salt buffer to stop the NSD2 enzymatic reaction. Cover the plate with TopSeal-A film and incubate 30 min at room temperature (r.t.) acceptor beads, biotinylated anti-H3 antibody and donor beads were then diluted in 1X detection buffer (PerkinElmer) before use. Acceptor beads/biotinylated antibody mix were then added at a final concentration of 20 µg/mL and 1 nM to the reaction mixture and the plate was incubated at r.t. for 1 h. Donor beads were added at a final concentration of 20 µg/mL and the plate was incubated at r.t. for 30 min in subdued light. The reaction was run in 384-well plates. The plates were read using an EnVision® reader. The resultant data were analyzed with graphPad prism.

Western Blot analysis. Total cellular extracts were lysed in buffer containing 2% SDS and quantified by the method of BCA protein assay. An equal amount of protein was subjected to electrophoresis on SDS-PAGE and transferred to nitrocellulose membranes, incubated with primary antibodies and then incubated with secondary antibody at room temperature for 1 h. Primary antibodies used were as follows: anti-beta-actin(Proteintech Group, 66009-1-Ig), anti-histone H3 (Cell Signaling

Technology, #9715) , anti-WHSC1/NSD2(abcam, ab75359), anti-Di-Methyl-Histone H3 (Lys36) (Cell Signaling Technology, #2901). The detection was performed using a SuperSignal west pico stable peroxide solution (Thermo Fisher Scientific).

Cell Proliferation Assay. The cell lines used in each experiment were obtained from the American Type Culture Collection. The cell line RS4:11, and KMS11 were cultured in the altered RPMI-1640 medium (Invitrogen) supplemented with 10% FBS (Gibco) and 2 mM lglutamine. The MV4:11 cell line was maintained in IMDM (Iscove's Modified Dulbecco's Medium) supplemented with 10% selected FBS (Gibco). For the cell proliferation assay, Cells were plated in 96-well plates at 6000-20000 cells per well in a volume of 200 μ L for 24 h. Then different concentrations of diluted compounds or DMSO added into the the cells and were cultured for another 6 d. Dosages corresponding to the half maximal inhibition (IC_{50}) were detected using the cell counting kit-8 (Life Technologies) according to the manufacturer's instructions.

Cell Cycle Analysis and Annexin V Staining. Cell cycle analysis was conducted by incorporating propidium iodide (PI). The cells were treated with 10 μ M, 5 μ M 033 or DMSO control for 48 h. Then cells were harvested and resuspended in PBS and fixed by 70% pre-cooled ethanol overnight. Then Cells were washed with PBS and resuspended in stain buffer containing 5 μ g/mL ribonuclease A (Sigma-Aldrich) and 5 μ g/mL PI for 45 min in room temperture for 40min. Acquisition was immediately performed on FACSCanto (BD Biosciences), and results were analyzed using modifit software.

Annexin V binding assay was used for apoptosis assay. The cells were cultured in 6 well plates at the optimal density. After 24h, different concentrations of the test compounds or DMSO control was added in the

plates for another 72h. Then 10^5 cells were collected and re-suspended in 100 μ L annexin V binding solution containing 0.25 μ g/mL anti-annexin V-FITC and 1 μ g/mL PI in the dark for 10 min. Samples were diluted with 400 μ L annexin V binding solution and analyzed by flow cytometry.

RNA Extraction and Real-time PCR. Total RNA was extracted with the EZ-press RNA Purification Kit (B0004DP) on the basis of manufacturer's prospectus. Reverse transcription was performed in a 20 μ L reaction volume with the total 2 μ g of RNA using HiScript II Q RT SuperMix (#R222-01, Vazyme, Nanjing, China). Real-time PCR were performed with SYBR Green Master Mix (#Q121-02, Vazyme) according to the manufacture's recommended protocol.

The following sequences of primers were designed to amplify PCR product:

GAPDH:

5'-GAGTCCACTGGCGTCTTCAC-3'

5'-TTCACACCCATGACGAACAT-3'

PAK1:

5'-GGTTTCAAGTGTTTAGTAACTTTTCCA-3'

5'-TTAGCTGCAGCAATCAGTGG-3'

RRAS2:

5'-GAGCAGCCCGGCTAGATATT-3'

5'-TGTTCTCTCATGGCTCCAAA-3'

TGFA:

5'-CCTGGCTGTCCTTATCATCAC-3'

5'-GGCACCCTCACAGTGTTTTC-3'

TEMEL2:

5'-CCACAGGGTTGCGTCTCAG-3'

5'-GGAGCACTGCACAGACAGAG-3'

HSPG2:

5'-CCAAATGCGCTGGACACATTC-3'

5'-CGGACACCTCTCGGAACTCT-3'

NCAM1:

5'-GGCATTTACAAGTGTGTGGTTAC-3'

5'-TTGGCGCATTCTTGAACATGA-3'

ASSOCIATED CONTENT

Supporting information

Molecular formula strings (CSV).

Diffraction data and structure refinement statistics of crystallography; extended data series for tested compounds (PDF)

Accession Codes

The PDB code for NSD2-PWWP1 bound with compound **5** is 7VLN. The authors will release the atomic coordinates and experimental data upon article publication.

AUTHOR INFORMATION

Corresponding Authors

Tongchao Liu – *Department of Medicinal Chemistry, Shanghai Institute of Materia Medica, Chinese Academy of Sciences, 555 Zuchongzhi Road, Shanghai 201203, P. R. China; Email: tongchao_liu@simm.ac.cn*

Xun Huang – *Division of Anti-tumor Pharmacology, State Key Laboratory of Drug Research, Shanghai Institute of Materia Medica, Chinese Academy of Sciences, Shanghai 201203, P. R. China; University of Chinese Academy of Sciences, Beijing*

100049, P. R. China; School of Pharmaceutical Science and Technology, Hangzhou Institute for Advanced Study, UCAS, Hangzhou 310024, P. R. China; Phone:+86 21 50806600; Email: xhuang@simm.ac.cn

Bing Xiong – Department of Medicinal Chemistry, Shanghai Institute of Materia Medica, Chinese Academy of Sciences, Shanghai 201203, P. R. China; University of Chinese Academy of Sciences, Beijing 100049, P. R. China; orcid.org/0000-0001-9776-8136; Phone: +86 21 50807088; Email: bxiong@simm.ac.cn

Shilin Xu – Drug Discovery & Development Center, State Key Laboratory of Drug Research, Shanghai Institute of Materia Medica, Chinese Academy of Sciences, #555 Zu Chong Zhi Road, Shanghai, 201203, China; University of Chinese Academy of Sciences, Beijing 100049, P. R. China; Email: slxu@simm.ac.cn

Authors

Na Li – Department of Medicinal Chemistry, Shanghai Institute of Materia Medica, Chinese Academy of Sciences, 555 Zuchongzhi Road, Shanghai 201203, P. R. China; University of Chinese Academy of Sciences, NO.19A Yuquan Road, Beijing 100049, P. R. China

Hong Yang – Division of Antitumor Pharmacology, State Key Laboratory of Drug Research, Shanghai Institute of Materia Medica, Chinese Academy of Sciences, 555 Zuchongzhi Road, Shanghai 201203, P. R. China

Ke Liu – Shanghai Synchrotron Radiation Facility, Shanghai Advanced Research Institute, Chinese Academy of Sciences, 239 Zhangheng Road, Shanghai 201210, China

Liwei Zhou – Department of Medicinal Chemistry, Shanghai Institute of Materia

Medica, Chinese Academy of Sciences, 555 Zuchongzhi Road, Shanghai 201203, P. R. China

Yuting Huang – *Division of Antitumor Pharmacology, State Key Laboratory of Drug Research, Shanghai Institute of Materia Medica, Chinese Academy of Sciences, 555 Zuchongzhi Road, Shanghai 201203, P. R. China*

Danyan Cao – *Department of Medicinal Chemistry, Shanghai Institute of Materia Medica, Chinese Academy of Sciences, 555 Zuchongzhi Road, Shanghai 201203, P. R. China*

Yanlian Li – *Department of Medicinal Chemistry, Shanghai Institute of Materia Medica, Chinese Academy of Sciences, 555 Zuchongzhi Road, Shanghai 201203, P. R. China*

Yaoliang Sun – *Drug Discovery & Development Center, State Key Laboratory of Drug Research, Shanghai Institute of Materia Medica, Chinese Academy of Sciences, #555 Zu Chong Zhi Road, Shanghai, 201203, China*

Aisong Yu – *Division of Antitumor Pharmacology, State Key Laboratory of Drug Research, Shanghai Institute of Materia Medica, Chinese Academy of Sciences, 555 Zuchongzhi Road, Shanghai 201203, P. R. China*

Zhiyan Du – *Department of Medicinal Chemistry, Shanghai Institute of Materia Medica, Chinese Academy of Sciences, 555 Zuchongzhi Road, Shanghai 201203, P. R. China*

Huan Zhou – *Shanghai Synchrotron Radiation Facility, Shanghai Advanced Research Institute, Chinese Academy of Sciences, 239 Zhangheng Road, Shanghai*

201210, China

Ying Zhang – *Division of Antitumor Pharmacology, State Key Laboratory of Drug Research, Shanghai Institute of Materia Medica, Chinese Academy of Sciences, 555 Zuchongzhi Road, Shanghai 201203, P. R. China*

Bingyang Wang – *Drug Discovery & Development Center, State Key Laboratory of Drug Research, Shanghai Institute of Materia Medica, Chinese Academy of Sciences, #555 Zu Chong Zhi Road, Shanghai, 201203, China*

Meiyu Geng – *Division of Anti-tumor Pharmacology, State Key Laboratory of Drug Research, Shanghai Institute of Materia Medica, Chinese Academy of Sciences, Shanghai 201203, P. R. China; University of Chinese Academy of Sciences, Beijing 100049, P. R. China; School of Pharmaceutical Science and Technology, Hangzhou Institute for Advanced Study, UCAS, Hangzhou 310024, P. R. China*

Author Contributions

N. L. designed and synthesized the compounds. H. Y. conducted the biological experiments and analyzed the results. K. L. resolved the co-crystal structure of NSD2-PWWP1 and compound **5**. L. Z. helped to design the molecules and synthetic route. These authors contributed significantly to this project, so we deemed them as equal contribution.

Y. S. and B. W. helped to design the molecules and synthetic route. D. C. and Y. L. conducted the enzymatic assay. Y. H., A. Y. and Y. Z. participated in the biological assays. D. C., Z. D. and H. Z. conducted the co-crystal structure of compounds with X-ray crystallography. M. G. helped to design the project.

N. L., H. Y. and K. L. prepared the initial manuscript. T. L., X. H., S. X. and B. X. designed the project and wrote the manuscript. All of the authors read and approved the final manuscript.

Notes

The authors declare no competing financial interest.

ACKNOWLEDGMENTS

We are grateful for financial support from the National Natural Science Foundation of China (Grant 21922707 and 81773572), the Major projects of National Natural Science Foundation of China (Grant 81991523), the Collaborative Innovation Cluster Project of Shanghai Municipal Commission of Health and Family Planning (Grant 2019CXJQ02), the Natural Science Foundation of Shanghai (21ZR1475500). Open Program of State Key Laboratory of new Drug development (Grant SIMM2105KF-04), SA-SIBS Scholarship Program and Shanghai Municipal Science and Technology Major Project. This work was carried out with the support of Shanghai Synchrotron Radiation Facility. We also thank Prof. Feng Yu and Prof. Jian Li for the assistance in determination of co-crystal structure.

REFERENCES

1. Vougiouklakis, T.; Hamamoto, R.; Nakamura, Y.; Saloura, V. The NSD family of protein methyltransferases in human cancer. *Epigenomics* **2015**, *7*, 863-74.
2. Bennett, R. L.; Swaroop, A.; Troche, C.; Licht, J. D. The Role of Nuclear Receptor-Binding SET Domain Family Histone Lysine Methyltransferases in Cancer. *Cold Spring Harb Perspect Med* **2017**, *7*.
3. Cheong, C. M.; Mrozik, K. M.; Hewett, D. R.; Bell, E.; Panagopoulos, V.; Noll, J. E.; Licht, J.

D.; Gronthos, S.; Zannettino, A. C. W.; Vandyke, K. Twist-1 is upregulated by NSD2 and contributes to tumour dissemination and an epithelial-mesenchymal transition-like gene expression signature in t(4;14)-positive multiple myeloma. *Cancer Lett* **2020**, *475*, 99-108.

4. Pierro, J.; Saliba, J.; Narang, S.; Sethia, G.; Saint Fleur-Lominy, S.; Chowdhury, A.; Qualls, A.; Fay, H.; Kilberg, H. L.; Moriyama, T.; Fuller, T. J.; Teachey, D. T.; Schmiegelow, K.; Yang, J. J.; Loh, M. L.; Brown, P. A.; Zhang, J.; Ma, X.; Tsigos, A.; Evensen, N. A.; Carroll, W. L. The NSD2 p.E1099K Mutation Is Enriched at Relapse and Confers Drug Resistance in a Cell Context-Dependent Manner in Pediatric Acute Lymphoblastic Leukemia. *Mol Cancer Res* **2020**, *18*, 1153-1165.

5. Chen, R.; Chen, Y.; Zhao, W.; Fang, C.; Zhou, W.; Yang, X.; Ji, M. The Role of Methyltransferase NSD2 as a Potential Oncogene in Human Solid Tumors. *Oncotargets Ther* **2020**, *13*, 6837-6846.

6. Sengupta, D.; Zeng, L.; Li, Y.; Hausmann, S.; Ghosh, D.; Yuan, G.; Nguyen, T. N.; Lyu, R.; Caporicci, M.; Morales Benitez, A.; Coles, G. L.; Kharchenko, V.; Czaban, I.; Azhibek, D.; Fischle, W.; Jaremko, M.; Wistuba, II; Sage, J.; Jaremko, L.; Li, W.; Mazur, P. K.; Gozani, O. NSD2 dimethylation at H3K36 promotes lung adenocarcinoma pathogenesis. *Mol Cell* **2021**.

7. Weinberg, D. N.; Papillon-Cavanagh, S.; Chen, H.; Yue, Y.; Chen, X.; Rajagopalan, K. N.; Horth, C.; McGuire, J. T.; Xu, X.; Nikbakht, H.; Lemiesz, A. E.; Marchione, D. M.; Marunde, M. R.; Meiners, M. J.; Cheek, M. A.; Keogh, M. C.; Bareke, E.; Djedid, A.; Harutyunyan, A. S.; Jabado, N.; Garcia, B. A.; Li, H.; Allis, C. D.; Majewski, J.; Lu, C. The histone mark H3K36me2 recruits DNMT3A and shapes the intergenic DNA methylation landscape. *Nature* **2019**, *573*, 281-286.

8. Yuan, S.; Natesan, R.; Sanchez-Rivera, F. J.; Li, J.; Bhanu, N. V.; Yamazoe, T.; Lin, J. H.; Merrell, A. J.; Sela, Y.; Thomas, S. K.; Jiang, Y.; Plesset, J. B.; Miller, E. M.; Shi, J.; Garcia, B. A.; Lowe, S. W.; Asangani, I. A.; Stanger, B. Z. Global Regulation of the Histone Mark H3K36me2 Underlies Epithelial Plasticity and Metastatic Progression. *Cancer Discov* **2020**, *10*, 854-871.
9. Huang, H.; Howard, C. A.; Zari, S.; Cho, H. J.; Shukla, S.; Li, H.; Ndoj, J.; Gonzalez-Alonso, P.; Nikolaidis, C.; Abbott, J.; Rogawski, D. S.; Potopnyk, M. A.; Kempinska, K.; Miao, H.; Purohit, T.; Henderson, A.; Mapp, A.; Sulis, M. L.; Ferrando, A.; Grembecka, J.; Cierpicki, T. Covalent inhibition of NSD1 histone methyltransferase. *Nat Chem Biol* **2020**, *16*, 1403-1410.
10. Bottcher, J.; Dilworth, D.; Reiser, U.; Neumuller, R. A.; Schleicher, M.; Petronczki, M.; Zeeb, M.; Mischerikow, N.; Allali-Hassani, A.; Szewczyk, M. M.; Li, F.; Kennedy, S.; Vedadi, M.; Baryte-Lovejoy, D.; Brown, P. J.; Huber, K. V. M.; Rogers, C. M.; Wells, C. I.; Fedorov, O.; Rumpel, K.; Zoephel, A.; Mayer, M.; Wunberg, T.; Bose, D.; Zahn, S.; Arnhof, H.; Berger, H.; Reiser, C.; Hormann, A.; Krammer, T.; Corcokovic, M.; Sharps, B.; Winkler, S.; Haring, D.; Cockcroft, X. L.; Fuchs, J. E.; Mullauer, B.; Weiss-Puxbaum, A.; Gerstberger, T.; Boehmelt, G.; Vakoc, C. R.; Arrowsmith, C. H.; Pearson, M.; McConnell, D. B. Fragment-based discovery of a chemical probe for the PWWP1 domain of NSD3. *Nat Chem Biol* **2019**, *15*, 822-829.
11. Coussens, N. P.; Kales, S. C.; Henderson, M. J.; Lee, O. W.; Horiuchi, K. Y.; Wang, Y.; Chen, Q.; Kuznetsova, E.; Wu, J.; Chakka, S.; Cheff, D. M.; Cheng, K. C.; Shinn, P.; Brimacombe, K. R.; Shen, M.; Simeonov, A.; Lal-Nag, M.; Ma, H.; Jadhav, A.; Hall, M. D. High-throughput screening with nucleosome substrate identifies small-molecule inhibitors of the human histone lysine methyltransferase NSD2. *J Biol Chem* **2018**, *293*, 13750-13765.
12. Ferreira de Freitas, R.; Liu, Y.; Szewczyk, M. M.; Mehta, N.; Li, F.; McLeod, D.;

Zepeda-Velazquez, C.; Dilworth, D.; Hanley, R. P.; Gibson, E.; Brown, P. J.; Al-Awar, R.; James, L. I.; Arrowsmith, C. H.; Barsyte-Lovejoy, D.; Min, J.; Vedadi, M.; Schapira, M.; Allali-Hassani, A. Discovery of Small-Molecule Antagonists of the PWWP Domain of NSD2. *J Med Chem* **2021**, *64*, 1584-1592.

13. Dilworth, D.; Hanley, R. P.; Ferreira de Freitas, R.; Allali-Hassani, A.; Zhou, M.; Mehta, N.; Marunde, M. R.; Ackloo, S.; Carvalho Machado, R. A.; Khalili Yazdi, A.; Owens, D. D. G.; Vu, V.; Nie, D. Y.; Alqazzaz, M.; Marcon, E.; Li, F.; Chau, I.; Bolotokova, A.; Qin, S.; Lei, M.; Liu, Y.; Szewczyk, M. M.; Dong, A.; Kazemzadeh, S.; Abramyan, T.; Popova, I. K.; Hall, N. W.; Meiners, M. J.; Cheek, M. A.; Gibson, E.; Kireev, D.; Greenblatt, J. F.; Keogh, M. C.; Min, J.; Brown, P. J.; Vedadi, M.; Arrowsmith, C. H.; Barsyte-Lovejoy, D.; James, L. I.; Schapira, M. A chemical probe targeting the PWWP domain alters NSD2 nucleolar localization. *Nat Chem Biol* **2021**.

14. Sankaran, S. M.; Wilkinson, A. W.; Elias, J. E.; Gozani, O. A PWWP Domain of Histone-Lysine N-Methyltransferase NSD2 Binds to Dimethylated Lys-36 of Histone H3 and Regulates NSD2 Function at Chromatin. *J Biol Chem* **2016**, *291*, 8465-74.

15. Wang, S.; Yang, H.; Su, M.; Lian, F.; Cong, Z.; Wei, R.; Zhou, Y.; Li, X.; Zheng, X.; Li, C.; Fu, X.; Han, X.; Shi, Q.; Li, C.; Zhang, N.; Geng, M.; Liu, H.; Li, J.; Huang, X.; Wang, J. 5-Aminonaphthalene derivatives as selective nonnucleoside nuclear receptor binding SET domain-protein 2 (NSD2) inhibitors for the treatment of multiple myeloma. *Eur J Med Chem* **2021**, *222*, 113592.

16. Wang, Q.; Yu, F.; Cui, Y.; Zhang, K.; Pan, Q.; Zhong, C.; Liu, K.; Zhou, H.; Sun, B.; He, J. Mini-beam modes on standard MX beamline BL17U at SSRF. *Rev Sci Instrum* **2017**, *88*, 073301.

17. Kabsch, W. Processing of X-ray snapshots from crystals in random orientations. *Acta Crystallogr D Biol Crystallogr* **2014**, 70, 2204-16.
18. Adams, P. D.; Afonine, P. V.; Bunkoczi, G.; Chen, V. B.; Echols, N.; Headd, J. J.; Hung, L. W.; Jain, S.; Kapral, G. J.; Grosse Kunstleve, R. W.; McCoy, A. J.; Moriarty, N. W.; Oeffner, R. D.; Read, R. J.; Richardson, D. C.; Richardson, J. S.; Terwilliger, T. C.; Zwart, P. H. The Phenix software for automated determination of macromolecular structures. *Methods* **2011**, 55, 94-106.
19. Kovalevskiy, O.; Nicholls, R. A.; Long, F.; Carlon, A.; Murshudov, G. N. Overview of refinement procedures within REFMAC5: utilizing data from different sources. *Acta Crystallogr D Struct Biol* **2018**, 74, 215-227.
20. Emsley, P.; Lohkamp, B.; Scott, W. G.; Cowtan, K. Features and development of Coot. *Acta Crystallogr D Biol Crystallogr* **2010**, 66, 486-501.

Table of Contents Graphic

Structure-based Discovery of NSD2-PWWP1 Inhibitors

